#5871

*Energy and Buildings*, *18* (1992) 101–131



# Wind pressure distribution around buildings: a parametrical model

Mario Grosso
*Department of Environmental Science and Technology, Politecnico di Torino, Turin (Italy)*

(Received June 1, 1990; accepted October 1, 1991; revised paper received November 16, 1991)

**Abstract**

This report describes the theoretical development of work done within the task group "wind pressure distribution" of the COMIS Workshop. The paper is divided into three Sections with an introductory part on the physical fundamentals. The first Section entails the objectives and the meaning of modelling wind pressure distribution as an integrated part of multizone airflow modelling. A literature review is presented, on calculation techniques and wind tunnel tests, and a description of the evaluation of an existing numerical model. The second Section is related to the development of the *Cp* calculation model. Objectives, characteristics and methodology of the parametrical approach chosen for the analysis are depicted, together with a description of the reference data, the regression technique, the algorithm, and the structure of the calculation model. The third Section is a detailed report of the results of the regression analysis. The curve-fitting process is explained with reference to the main factors affecting the wind pressure distribution on a building envelope: terrain roughness, surrounding buildings, aspect ratios, and wind direction. Figures of the curves are shown. In the Appendix, equations and relevant coefficients of the curve-fitting are presented.

## 1. Introduction

The wind pressure distribution around a building is an important parameter for multizone airflow simulation. Current multizone air infiltration models generally deal with pressure coefficients as an input, regardless of the technique used to provide the data.

Since the beginning of the COMIS Workshop, the development of a *Cp* calculation procedure as an integrated module of the COMIS model has been considered an essential task. The aim of the module was to provide local, not wall-averaged, *Cp* data in relation to the context parameters of the building under analysis, i.e., meteorological and environmental conditions of the site, and geometrical characteristics of the building. The *Cp* calculation module was planned to deal with a continuous variation range of those parameters within limits defined by the characteristics of the experimental data to be used as reference for the regression analysis.

After a broad literature review, both on wind tunnel tests and *Cp* calculation techniques, the decision to develop a new algorithm was made. An existing algorithm was considered and checked, but it did not meet the desired requirements. A parametrical approach was chosen as the most suitable to develop a simple algorithm with the available reference data found in the literature review.

### *1.1. Physical fundamentals*

Wind pressure is one of the two main driving forces for natural ventilation. Differences in the temperature of the earth surface due to solar radiation cause global pressure differences in the atmosphere. Compensation for these pressure differences causes the flow of enormous amounts of air from regions of high pressure to regions of low pressure. The direction of this airflow, i.e., wind, depends on the pressure gradient, Coriolis force, and friction on the earth's surface.

The shear layer formed by the action of shear stress at a solid boundary is called the boundary layer. The velocity in the shear layer goes from zero at the surface of the solid boundary up to the velocity of the free stream at the outer edge. The flow in the region between both limits is dominated by the effect of viscosity. Depending upon the Reynolds number, the flow in this region is either laminar or turbulent. Wind flow is characterized by turbulent boundary layer flow with a thickness of a few hundred metres [1, 2].

0378-7788/92/$5.00

When a boundary layer flow hits a sharp edge, such as a corner of a rectangular building, separation occurs immediately. The effect of the Reynolds number is negligibly small for rectangular buildings, because it is no longer the dominating factor in controlling the separation and wake width [3].

The vertical profile of the wind speed in the atmospheric boundary layer is primarily dependent upon the roughness of the surface surrounding the building. The wind speed increases with increasing height above ground. The mean wind velocity profile can be calculated either by a logarithmic equation [4]:

$$\frac{v(z)}{v(z_{\mathrm{ref}})} = \frac{\ln(z-d) - \ln z_0}{\ln(z-d)_{\mathrm{ref}} - \ln z_{0_{\mathrm{ref}}}} \tag{1}$$

or a power law expression [5]:

$$\frac{v(z)}{v(z_{\mathrm{ref}})} = \left\{\frac{z}{z_{\mathrm{ref}}}\right\}^{\alpha} \tag{2}$$

For structural purposes the exponential or power law profile has been used most widely because of its simplicity [6, 7]. The logarithmic equation is less empirical, allowing for calculation of both terrain roughness and zero flow plane displacement and thereby having a better standard deviation from measured values [8–11].

Both equations assume that the wind flow is isothermal and horizontal. An assumption is made that the wind flow will not change its direction as a result of differences in the terrain surface. The value of the exponent $\alpha$ increases with increasing roughness of the solid boundary. Figure 1 shows the wind profile for three selected types of surrounding roughness.

In areas with relatively homogeneous roughness, eqns. (1) and (2) are valid for a height above the obstacles corresponding to the whole boundary layer thickness. For smaller areas of rough surfaces in a more smooth surrounding, such as a town located in flat, open surroundings, the velocity profile described by eqns. (1) and (2) is only valid for a limited height above the obstacles. The wind velocity well above the small town is determined by the roughness of its surroundings which is very different, in this case, from the one of the town itself. The wind velocity profile for the entire thickness of the boundary layer above the town can be discontinuous, being in fact the combination of two different profiles. Some standard values for $\alpha$ and for the boundary layer thickness are shown in Table 1 [13].

Wind flows produce a velocity and pressure field around buildings. The relationship, for free stream flow, between velocity and related pressure at different locations of the flow field can be obtained from Bernoulli's equation. Assuming constant density along a streamline at a given height, Bernoulli's equation can be simplified to:

$$P_{\mathrm{stat}} + \frac{1}{2}\rho\bar{v}^2 = \mathrm{const} \tag{3}$$

The wind pressure distribution on a building's envelope is usually described by dimensionless pres-

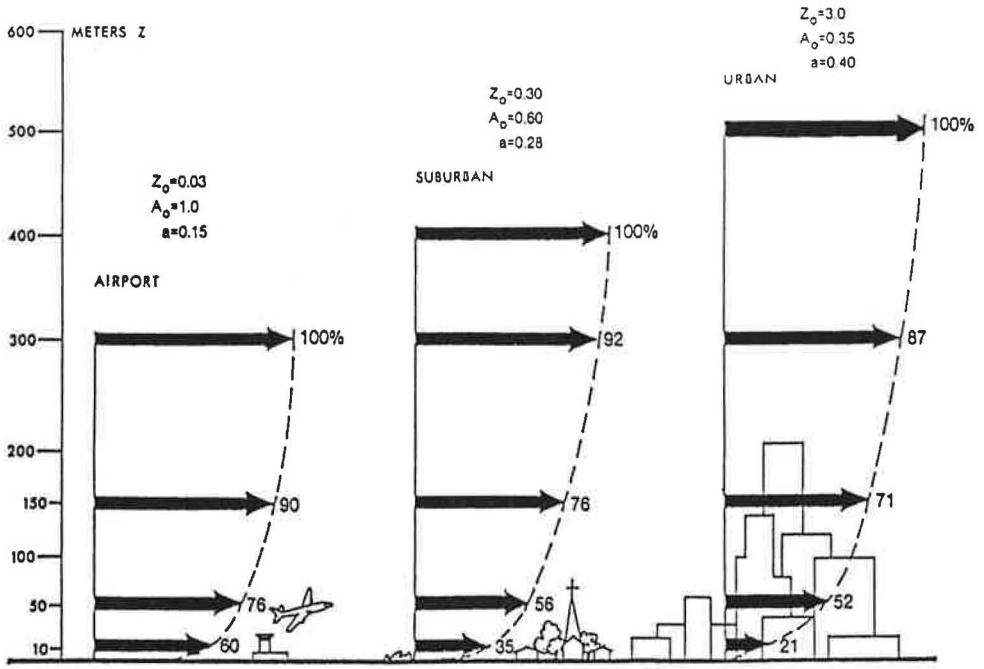


Fig. 1. Mean wind velocity profiles [12].

TABLE 1. Height of boundary layer and exponents for different surrounding roughness [13]

| Roughness type | Height of boundary layer (m) | Exponent $\alpha$ (–) |
|---|---|---|
| Flat open country | 270 | 0.14 |
| Rolling hills | 390 | 0.28 |
| Inner city areas | 510 | 0.40 |

sure coefficients – the ratio of the surface dynamic pressure to the dynamic pressure in the undisturbed flow pattern measured at a reference height. The pressure coefficient $Cp$ at point $k(x, y, z)$, with the reference dynamic pressure $P_{dyn}$ corresponding to height $z_{ref}$, for a given wind direction $\phi$ can be described by:

$$Cp_k(z_{ref}, \phi) = \frac{P_k - P_0(z)}{P_{dyn}(z_{ref})} \tag{4}$$

with

$$P_{dyn}(z_{ref}) = \frac{1}{2} \rho_{out} v^2(z_{ref}) \tag{5}$$

## 2. Modelling wind pressure distribution

### 2.1. Introduction

There are a number of variables affecting the pressure distribution around a building due to natural wind. Wall-averaged values of $Cp$ usually do not match the accuracy required for multizone airflow calculation models. More detailed evaluations, taking the $Cp$ distribution on the envelope of buildings into account, can be made according to different approaches:

- performing full-scale measurements when an existing building is being studied;
- carrying out wind tunnel tests on models of existing or designed buildings;
- generating $Cp$ values by 3-dimensional numerical airflow models;
- generating $Cp$ values by numerical models based on parametrical analysis of wind tunnel test results.

The first approach is practically impossible to follow, unless it is done within expensive and time-consuming experimental plans. The second approach depends on the availability of test equipment and relevant assistance. The third approach implies time-consuming and complex calculations. The fourth approach seems to assure easy access to available $Cp$ data by using a simple algorithm.

The wind pressure distribution (*wpd*) model described in this paper belongs to the fourth category. It combines detailed measured results with the generality of the application.

Modelling *wpd* means finding an algorithm to calculate the variation of $Cp$ on the envelope surfaces of a building when varying wind direction, architectural and environmental conditions. Because of the stochastic behaviour of the wind pressure distribution around a building, such an algorithm has to be drawn by empirical correlations, which hold only within the range of variation of the experimental reference data used for the analysis.

Unlike wall-averaged values of $Cp$, where tables and graphs are given for wide intervals of wind angle [14, 15], a *wpd* model can yield $Cp$ values at any point on the surface for any specific wind angle.

On the other hand, unlike wind tunnel or full-scale tests on a specific building-site situation, a *wpd* model has a high abstraction level, having to match a wide range of climatic and environmental conditions. Nevertheless, a *wpd* model can approach the actual flow pattern with relatively high accuracy depending upon the characteristics of the data on which it is based.

The following is a description of the work carried out to develop a *wpd* model able to perform $Cp$ calculations in basic general boundary conditions, and characterized by a modular structure allowing for further upgrading. As a first step, a literature review was undertaken both on *wpd* models and wind tunnel tests.

### 2.2. Literature review

#### 2.2.1. Models

Although numerous papers on wind pressure have been published [16, 17], only a few contribute to the *wpd* modelling.

Allen [18] described a calculation method showing how the variation of pressure coefficients with wind angle can be represented by a Fourier series. Results are shown only for whole-face-averaged $Cp$ except for a location at relative building height 0.85 where horizontal distribution is plotted in relation to a specific environmental situation. In addition, the dependence of Fourier series on side ratio and shelter is demonstrated. The publication mentions the necessity of further investigation, mainly concerning the fluctuating pressures arising from turbulence, different building shapes, and the sheltering effect of neighbouring buildings.

Bala'zs [19] developed a software package called CPBANK, which includes a set of $Cp$ data files for different predefined building geometries and ex-

posures. A program performs the search of *Cp* values for a selected set of wind directions related to any building similar to CPBANK types. The reference data are taken from a series of results of tests performed in the Wind Tunnel Laboratory of the Hungarian Institute of Building Science (ETI).

Swami and Chandra [20] performed a survey with the objective "...to review the worldwide data on building pressure coefficient and to assimilate the data for use in hourly calculations of natural ventilation airflow rates in buildings". For low-rise buildings, data from eight different investigators were analyzed. It was found that average surface pressure coefficients were adequate. Local data were assimilated as 544 average surface pressure coefficients. A non-linear regression with wind incidence angle (*anw*, see definition in Section 4.4) and building side ratio — the ratio of the length to the width of the building — as variables was found to predict these data with a correlation coefficient of 0.80. The surveyed *Cp* data were converted with respect to the wind velocity at the model height using the boundary layer profile characteristics extracted from the references. In order to simplify the calculation, values of *Cp* at different wind angles were normalized with respect to *Cp* at wind angle 0 (perpendicular to the windward wall). The reference *Cp* values for zero incidence were found "...highly diverse, showing no firm trend with respect to any parameter whatsoever," and "...an attempt to correlate such diverse set of data would prove futile due to inherent characteristics of the experiment of each researcher" [20, 2–17]. In light of the above, a uniform value of 0.60 was chosen to represent the average *Cp* at zero incidence for all types of low-rise buildings.

For high-rise buildings, local pressure coefficients taken from Akins [22] and related to models of different sizes (see Section 2.2.2) were used. More than 5000 data points were fitted to another non-linear regression involving the earlier variables plus the location coordinates. The *Cp* data from Akins are referenced with respect to the velocity at the height of measurement (local *Cp*) and, therefore, are independent on either terrain roughness or height of the building. For this reason, Swami and Chandra [20] made no attempt to normalize the *Cp* data and the actual data were fitted. The data set was split into five categories based on side ratios of 1.0, 2.0, 4.0, 0.25, and 0.5. With the side ratio eliminated as a parameter, these five data sets were independently analyzed for the other parameters, namely wind angle and surface location (*xl* and *zh*, see Fig. 21). A large number of runs were carried out to get similar variables to fit all five data sets. Five equations differing only for the values of the regression coefficients were obtained with correlation coefficients varying from 0.88 to 0.92. Once the regression coefficients were obtained for each of the five sets of data, the regression coefficients were themselves analyzed for dependence on the side ratio. Once the functional form of the side ratio was obtained, new parameters were developed from the combination of wind incidence angle, *xl*, *zh*, and side ratio, reflecting these functional forms and the new parameters were used as input to curve-fit the entire data of Akins. The highest value for the correlation coefficient obtained was 0.89.

### 2.2.2. *Wind tunnel tests*

Among several wind tunnel tests, those dealing with a wide variation range of one or more parameters were considered, and three of them were analyzed in more detail in order to find sample data sets to be used for evaluating one of the models described above as well as for developing new calculation routines.

Hussein and Lee [21] measured surface pressure coefficients on block-shaped models of different size, with different surrounding layout patterns and densities, and with only one wind direction, in an atmospheric boundary layer wind tunnel. Models of different size and height were tested and the results were related to the results obtained for a cube-shaped model with 0.036 m side corresponding to a dimension of 12.6 m in real scale (1:350). Models 0.036 m high, 0.036 m wide (facade parallel to the flow), and with length (facade facing the flow) 0.5, 1.5, 2.0, 4.0 times the height were used to test the variation of *Cp* with frontal aspect ratio (see definition in Section 4.3). Analogously, models 0.036 m high, 0.036 m long, and with width 0.5, 1.5, 2.0 times the height were used to test the variation of *Cp* with side aspect ratio (see definition in Section 4.3). Square-plan models with 0.036 m plan side and height varying within a range of 0.5–4.0 times the plan side were used in order to test the variation of *Cp* with height ratio. *Cp* was measured along the vertical centreline of the windward and leeward facades of each model with approaching flow normal to the facades. Eight pressure tappings were used on the models 0.036 m high, and a number of tappings ranging from 5 to 15 on the models with varying height. Pressure coefficients were normalized with respect to the velocity of the gradient wind which, in their case, occurred at a height of 22 times the cube height. They provided a wind velocity profile with a flow exponent $\alpha = 0.28$ to simulate the atmospheric wind flow in a low density urban area.

Akins and Cermak [22] performed their test in an industrial aerodynamic wind tunnel measuring surface pressure coefficients at several points on the facades of 15 block-shaped models of different size. The whole set of models can be sorted in three bins with regard to their side ratio: 1.0 (square plan), 0.5, and 0.25. Each group includes five models with width (the smaller of the plan sides) and height, respectively, of 0.032, 0.064, 0.127, 0.127, 0.254, and, 0.254, 0.254, 0.254, 0.508, 0.254 m. According to an average scaling factor of 1:250 amid the four boundary layers tested, the five basic model sizes correspond to full-scale sizes of 8.0, 16.0, 31.75, 63.5, and 127 m. The effect of the immediate surroundings was not simulated. Five different wind incidence angles on each wall ($anw = 0°$, 20°, 40°, 70°, 90°) and four terrain roughness types ($\alpha = 0.12$, 0.26, 0.34, 0.38) were tested. Pressure coefficients were measured both in vertical and horizontal distribution and normalized with respect to the local wind velocity. The *Cp* data are presented in the form of "averaged mean local pressure coefficients" in 75 tables: five, representing the four facades and the roof, for each wind incidence angle and for each side ratio. The *Cp* values at each grid location (spacing 0.1 the length and the height of each facade) were obtained by averaging the values of the mean local pressure coefficient belonging to the group of models with the same side ratio for all model heights and for all boundary layers. The authors acknowledge that "some effects are overlooked in this type of condensation, but such a technique was the only realistic method of presenting the volume of data collected" [22, p. 66]. In addition to the averaged data shown in the report, three sets of data related to a cube-shaped model with 0.254 m side and for terrain roughness corresponding to $\alpha = 0.12$, 0.34, 0.38 were obtained from the authors.

Bowen [23] performed his test in an aeronautical wind tunnel measuring *Cp* at different points on walls and roofs of rectangular-shaped models. These were $0.114 \times 0.076$ m as plan, $45.7 \times 30.5$ m in real scale, and had modular height of 0.5, 1, 2, 3 times the width (0.076 m). The test was referred to a boundary layer condition typical of a high density urban area ($\alpha = 0.43$) without evaluating the nearby surrounding effect.

### 2.3. *Evaluation of an existing model*

Swami and Chandra's equation for low-rise buildings calculates average surface pressure coefficients. Since the aim of the present work was to develop a computer model yielding *Cp* values at any specific location on a building wall — as needed to calculate infiltration and ventilation in multistorey buildings — that equation could not be used. Instead, the possibility of using Swami and Chandra's equation related to high-rise buildings as an algorithm for the *Cp* calculation model was evaluated and the equation was checked by applying it to sample models taken from the wind tunnel tests. Output data from Swami and Chandra's model were compared to *Cp* data from Hussein and Lee, and Akins and Cermak. The data relate to a range of common parameters used in the two tests: terrain roughness ($0.26 < \alpha < 0.28$), wind incidence angle ($anw = 0°$), side ratio (1, square-plan model), horizontal location on the facade ($xl = 0.5$), and vertical location on the facade ($0.0 \leqslant zh \leqslant 1.0$, by 0.1).

The boundary layer thickness is used as the reference height for the wind velocity in Hussein and Lee's test while the vertical location of each considered facade element is the reference height for the wind velocity in Akins and Cermak's test as well as in Swami and Chandra's model. A conversion of all three data sets to the model height as a new common reference for the wind velocity was made in order to compare them. This conversion was made using the definition of surface pressure coefficient (see eqn. (4)). If $Cp_k$ is a specific value of the surface pressure at the location $k$ with reference wind velocity at $z_{\text{ref}}$, wind direction $\phi$, and velocity profile exponent $\alpha$, a new value $Cp'_k$ for the same dynamic pressure, referenced at $z'_{\text{ref}}$, with wind direction $\phi$, and velocity profile exponent $\alpha'$, can be calculated by proper manipulation of eqns. (2), (4) and (5):

$$Cp'_k(z'_{\text{ref}}\phi) = Cp_k(z_{\text{ref}}\phi)\left\{\frac{z^{(\alpha'-\alpha)}}{z'^{\alpha'}_{\text{ref}} z^{-\alpha}_{\text{ref}}}\right\}^2 \qquad (6)$$

As Fig. 2 shows, the profile calculated by Swami and Chandra's equation matches that of Akins and Cermak at $zh = 0.7$ and that of Hussein and Lee at $zh = 0.2$. Within this interval, the *Cp* value is always greater than the sample values. Outside of this interval, the *Cp* values are in between the two sample profiles, except in the case of $zh < 0.1$. With the exception of the very bottom ($zh < 0.1$) and the very top ($zh > 0.9$) of the facade, the deviation of Swami and Chandra's profile from the average values between the two samples is never greater than 10%, tending toward an over-evaluation of *Cp*. The difference between the profile drawn from Swami and Chandra's model and the one from Akins and Cermak's test, in spite of the fact that the former used the latter as reference data set, is due to the different regression technique used: Akins and Cermak's profile shown in Fig. 2 is based on eleven values of

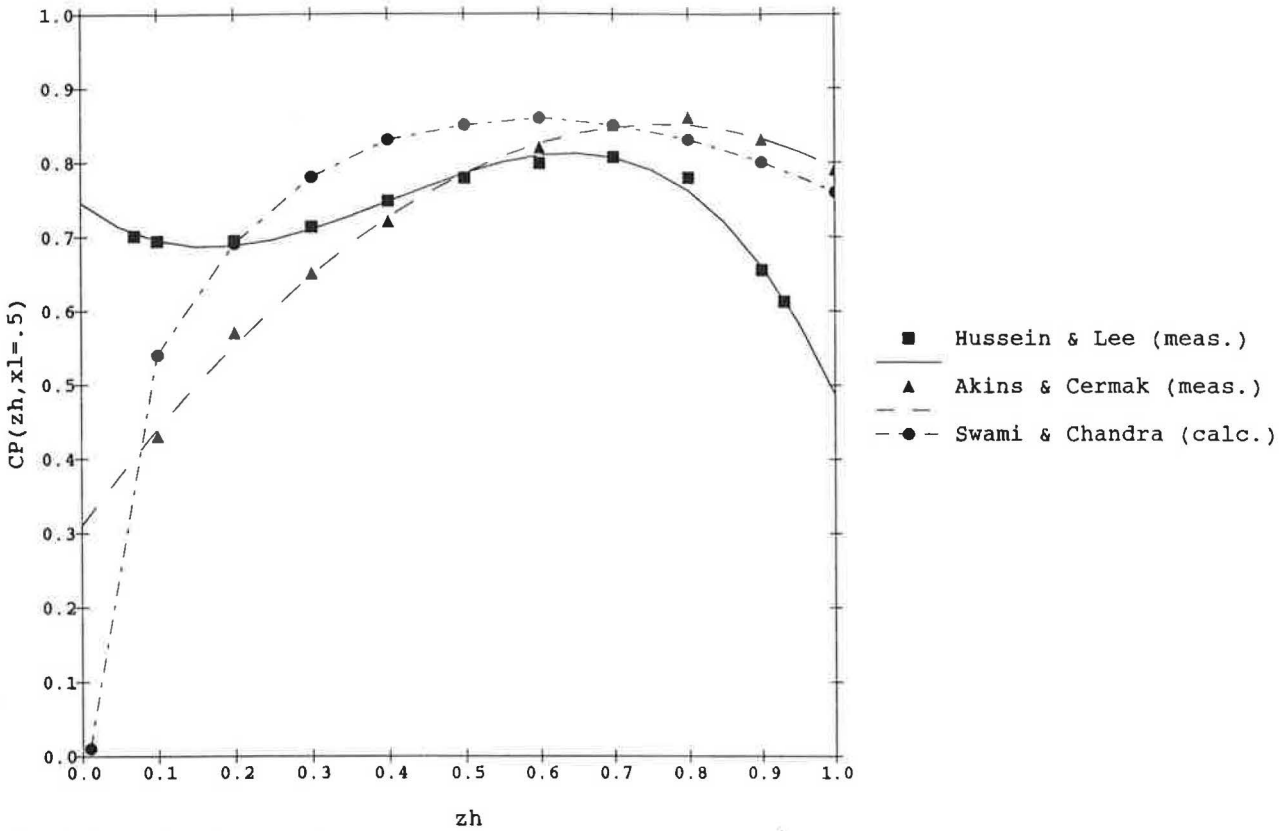


Fig. 2. Comparison between Swami and Chandra's model and wind tunnel tests — centreline vertical profile.

*Cp* and was obtained by curve fitting which uses a second-degree polynomial with a correlation factor of 0.99; Swami and Chandra's profile is calculated by a model developed with a more complex regression method based on a much greater number of data (see Section 2.2.1).

The second comparison was made between the output of Swami and Chandra's model and Akins and Cermak's data set related to horizontal *Cp* profiles. The evaluation was made for three wind incident angles, 0°, 45° and 90°, at $zh = 0.7$, where *Cp* from the model and *Cp* from the test matched in the previous check. In this comparison (Fig. 3), the sample profiles look very different from Swami and Chandra's profiles. While the data are close to each other at the centre of the facade, they are very different along the horizontal line. The reason for this discrepancy could be the same as given for the previous comparison. The wrong asymmetry in the case of normal wind can be attributed to a mistake in the report version.

Owing to the different parameters used to calculate the shielding effect of the immediate surroundings by Swami and Chandra and by Hussein and Lee (Akins and Cermak did not consider it), no check related to this effect could be carried out. Hussein and Lee took various densities and two layout patterns of the surroundings into account and their effect on *Cp* was measured on each tap of all models considered in the test. Swami and Chandra did not include those parameters in their equation. In the case where the surrounding layout matches one of the three configurations defined by Wiren [15] — normal pattern, hexagonal pattern, single neighbouring building — a surface average correction factor for each configuration can be added to the *Cp* value as calculated by the model. Three linear equations as functions of the wind angle are given to calculate these correction factors. In the case where the surrounding pattern does not match any of the cases mentioned above, correction factors are suggested to the ventilation flow rate in relation to five shielding classes.

The conclusion of the overall test was that the Swami and Chandra algorithm, though valuable for estimates either of surface average pressure coefficients on low-rise buildings or of *Cp* along the vertical centreline on a facade of an isolated high-rise building in the case of normal approaching wind and suburban terrain roughness, would not be able to fulfil the wider needs of the multizone infiltration model being developed.

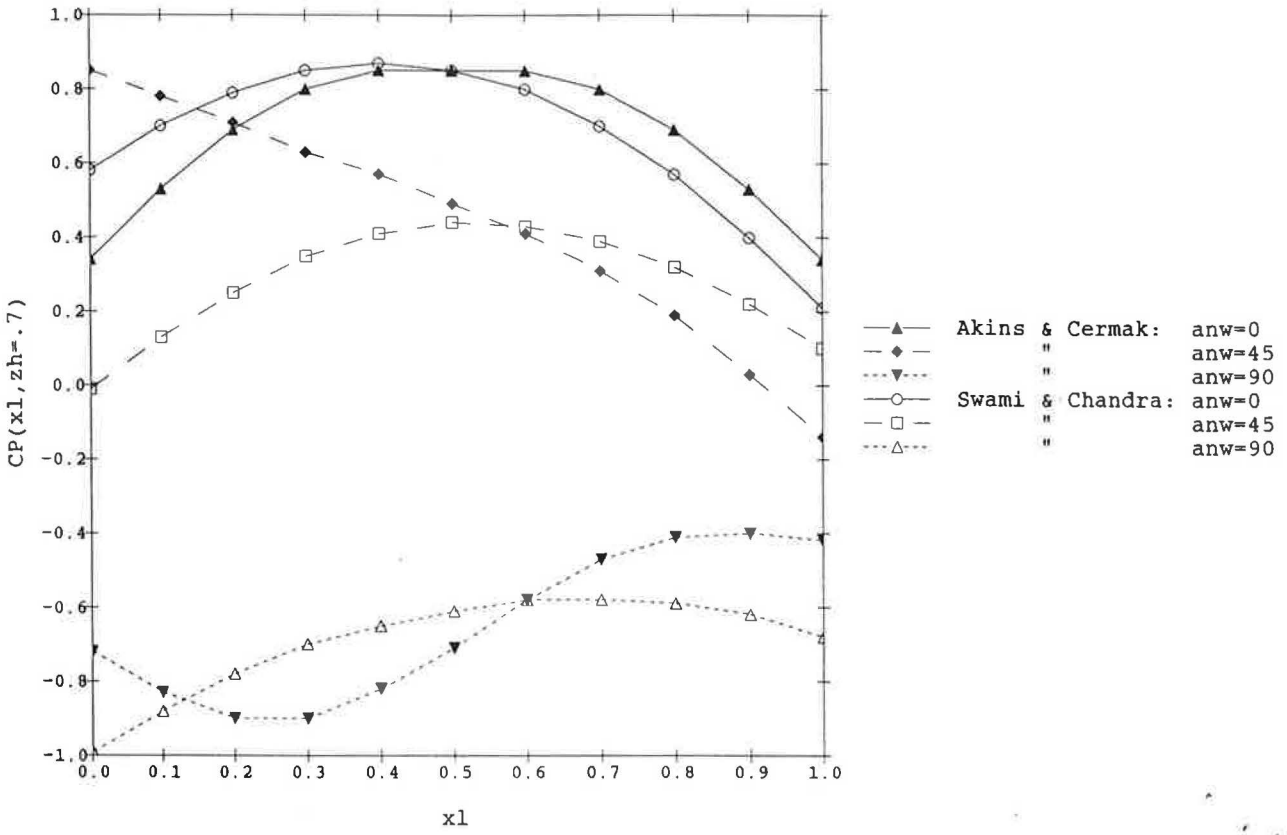


Fig. 3. Comparison between Swami and Chandra's model and wind tunnel tests – horizontal profile.

## 3. Model development

### *3.1. Introduction*

A model was developed by analyzing data from wind tunnel tests using a parametrical approach. This means using a systematic analytical process in which each parameter influencing the variation of a factor is considered as an independent variable while the others are kept constant. Variation curves for each parameter, using statistical regressions, are then defined and the effect on the analyzed phenomenon, e.g., wind pressure distribution, evaluated. The assumption is made that the influence of the variation of a parameter upon another is not greater than the average standard deviation of the whole regression process.

For the present analysis three types of parameters were taken into account:

- *climate parameters*

– wind velocity profile exponent ($\alpha$, see eqn. (2))
– wind incident angle (*anw*, see Section 4.4, Fig. 22);

- *environment parameters*

– plan area density (*pad*, see Section 4.2, Fig. 10)
– relative building height (*rbh*, see Section 4.2);

- *building parameters*

– frontal aspect ratio (*far*, see Section 4.3)
– side aspect ratio (*sar*, see Section 4.3)
– relative vertical position (*zh*, see Section 4.4, Fig. 21)
– relative horizontal position (*xl*, see Section 4.4, Fig. 21).

The specific objective was to find the relationship between variation range of each parameter and change of *Cp* on a rectangular-shaped building model in order to develop calculation routines as input for a multizone infiltration and ventilation model.

### *3.2. Reference data*

Among the wind tunnel tests analyzed in the literature review, two were selected as reference, on the basis of the following features:

- number of parameters considered in the tests;
- range of values for each parameter;
- similarity of parameter values between the two tests;
- lack of other experimental data on the parameters analyzed by Hussein and Lee (*pad*, *rbh*).

The data sets for analyzing the parameters *pad*, *far* and *sar*, *rbh*, were taken from the three in-

vestigations carried out by Hussein and Lee [24–26] and dealing, respectively, with:

- a cube-shaped model changing plan area density (13 values from 3.125 to 50) both on normal and staggered layout patterns;
- models of different plan forms (see description in Section 2.2.2) and with at least 15 densities (normal layout pattern) for each considered aspect ratio;
- models of different relative height with respect to the height of an isolated cube-shaped model and to the height of surroundings blocks with four values of plan area density in normal as well as staggered layout patterns;

The parameters considered in Akins and Cermak's test (see description in Section 2.2.2) are:

- horizontal distribution (parameter $xl$), eleven values from 0 to 1 by 0.1;
- wind direction ($anw$), 0°, 20°, 40°, 70°, 90°, corresponding to nine wind incidence angles (from 0° to 180°) for each facade;
- velocity profile exponent ($\alpha$), four values related to the following terrain roughness types:

$\alpha = 0.12$ level surface with very small obstructions, grassland

$\alpha = 0.26$ rolling or level surface broken by numerous obstructions such as trees or small houses

$\alpha = 0.34$ heterogeneous surface with structures larger than one storey

$\alpha = 0.38$ heavily built-up metropolitan area.

Parameter values common to the two tests are:

$0.26 \leqslant \alpha \leqslant 0.28$

$0.07 \leqslant zh \leqslant 0.93$

$xl = 0.5$

$anw = 0$, $anw = 180$.

This range of common values corresponds to the $Cp$ centreline vertical profile on the windward and leeward facades of a model with approaching wind normal to the facades in a boundary layer typical of a suburban area. It was taken as reference for the regression analysis as well as for the calculation model after conversion to the height of the model as a new reference for the wind velocity (see Section 2.3). The allocation of the reference data within the analysis framework is shown in Fig. 4 where the values of the parameters are related to the windward facades. For the leeward facades, the only variation is the parameter $anw = 180$.

As shown in Fig. 4, the aspect ratio (AR) of Hussein and Lee's reference model (cube) is different from the "average" Akins and Cermak model used as reference to analyse the effect of wind direction due to the condensed way in which the data are presented in Akins and Cermak's report (Section

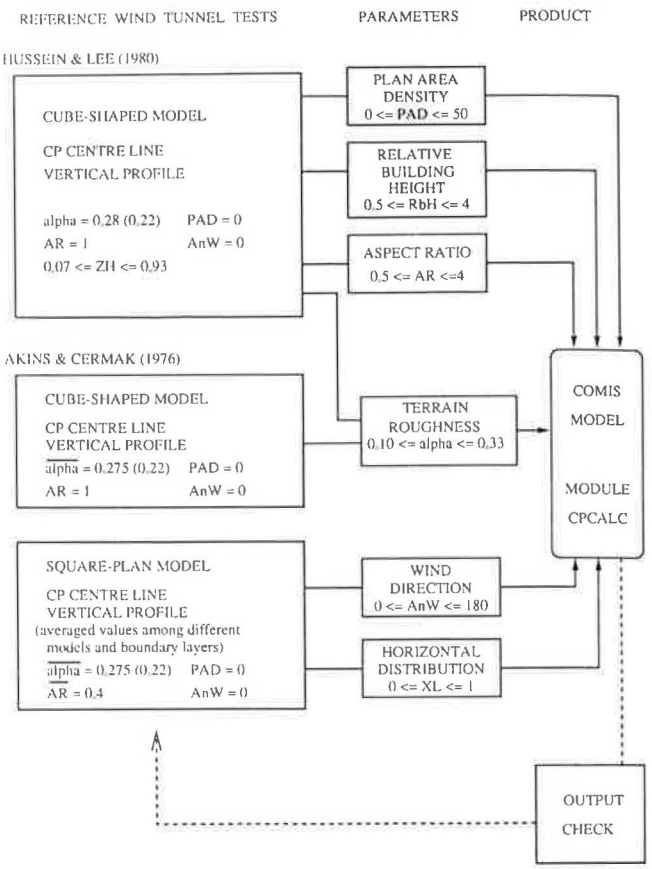


Fig. 4. Allocation of the reference tests within the analysis framework.

2.2.2). A correction factor was applied to Akins and Cermak's data set in order to compare it to Hussein and Lee's reference profile. The correction factor was derived from the analysis of the variation of $Cp$ with aspect ratios (see Section 4.3.).

As shown in Fig. 5, the two $Cp$ profiles are reasonably similar considering the non-identical conditions of the two tests, particularly the real size of the models. With the above correction, the two profiles were used as reference for the regression analysis (Sections 3.3.1, 3.3.2) for the windward vertical facades. The same procedure was used for the leeward vertical facades.

The reference profiles are defined, analytically, as functions of $zh$ for the following values of the other parameters here considered as independent variables:

$\alpha = 0.28$ (corrected to 0.22 as explained in Section 4.1), $pad = 0.0$, $rbh = 1.0$, $far = 1.0$, $sar = 1.0$, $anw = 0°$ (windward), $anw = 180°$ (leeward), $xl = 0.5$.

Hussein and Lee's profiles were taken as reference for the calculation model based on the assumption that the $Cp$ horizontal distribution does not change

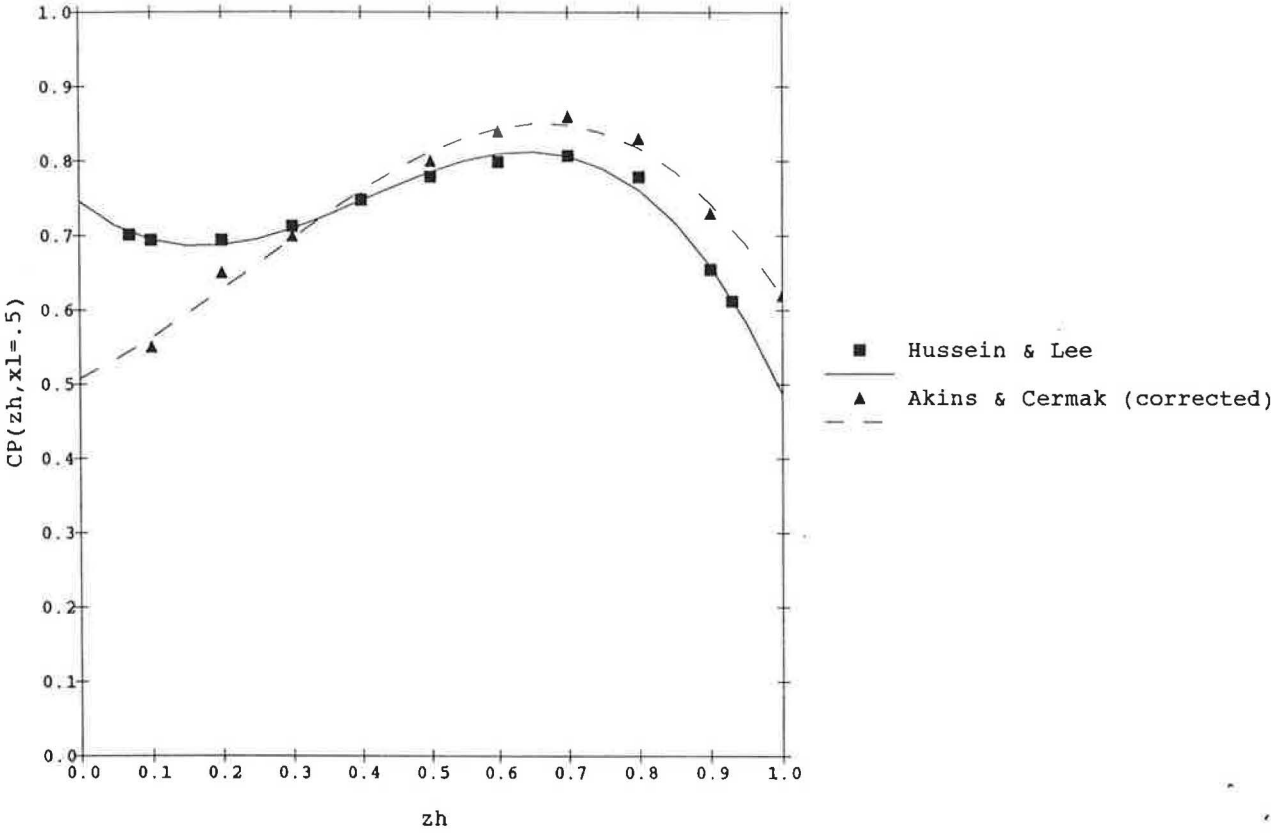


Fig. 5. Reference *Cp* centreline vertical profiles — windward wall.

with plan area density, relative building height, aspect ratios and wind velocity profile exponent.

### 3.3. Methodology

The method used to analyse and to fit the *Cp* data from the reference tests and to develop an algorithm for the computer model is based on the following criteria:

- consistency with the data structure and with the experimental setting conditions;
- consistency with the parametric approach described above;
- simplicity and accuracy of the regression technique (correlation coefficient. $>0.95$);
- simplicity of the algorithm;
- consistency of the algorithm with the characteristics of a modular model.

The whole process includes the regression analysis of the *Cp* data, the development of the algorithm, and the writing of the calculation model.

#### 3.3.1. Regression technique

The regression analysis was carried out using the statistical software RS/1 [27]. The reference *Cp* profiles were fitted to a polynomial function:

$$CP_{ref}(zh) = a_0 + a_1(zh) + a_2(zh)^2 + \ldots\ldots a_n(zh)^n \qquad (7)$$

where

$0.07 \leqslant zh \leqslant 0.93$ (Hussein and Lee)

$0.0 \leqslant zh \leqslant 1.0$ (Akins and Cermak)

$n = 3$ (windward facade)

$n = 5$ (leeward facade).

All the other data were analysed not in their actual value but as normalized *Cp* values. Normalization for each parameter was done, with respect to the *Cp* corresponding to the reference value of the parameter (see Section 3.2). The main reasons for this approach are described as follows.

- Since both reference tests have a different reference height for the wind velocity from the one chosen for the calculation model, dealing with normalized values allowed for the majority of the data to be analyzed with their original reference.
- Setting and model sizes of the two tests are different. Normalized *Cp* values take the range of variation of *Cp* for each parameter into account rather than the actual *Cp* and, therefore, allow for considering the two data sets as a whole as long as the relevant reference values are reasonably close to each other as shown in Fig. 5.
- Hussein and Lee's data are shown as vertical profiles along the centreline of the windward and leeward facades of the models, while Akins and Cermak's are tabulated for the vertical as well as

the horizontal distribution on each facade. The normalization of *Cp* allows for the selection of a parameter as an independent variable common to the two sets of data which in this case is *zh*.

• Such a technique implies that the whole set of data in each test be sorted into relatively small groups of data allowing for a high correlation factor in the curve-fitting.

The *Cp* data were sorted into the following groups of parameters:

*α* (3), *zh* (5) terrain roughness;
*pad* (13), *zh* (11) density of surrounding buildings;
*rbh* (8), *pad* (4), *zh* (11) ratio of model height to height of surrounding buildings;
*far* (4), *pad* (5), *zh* (6) frontal aspect ratio;
*sar* (3), *pad* (5), *zh* (6) side aspect ratio;
*anw* (5), *xl* (1), *zh* (10) wind direction (*Cp* vertical centreline);
*xl* (11), *anw* (10), *zh* (3) wind direction (*Cp* horizontal distribution);

The first symbol in each group represents the dependent variable for which a regression function was to be found; the second symbol – and the third symbol, if present – represents the independent variable at a specific value of which the *Cp* value was measured. The number in parenthesis is the number of measurement points taken for each parameter in the case of windward facades (a total of 1100 *Cp* data were analysed for the windward facades; a slightly smaller number for the leeward facades).

The data in each group were normalized with respect to the reference value of the dependent variable for each value(s) of the independent variable(s). If $Cp_{i_n, j_m}(d_t)$ is a generic value of *Cp* corresponding to the $n$, $m$ and $t$ values of $i$, $j$, and $d$ – any of the above-mentioned parameters in relation to their position, respectively, as an independent ($i$, $j$) or dependent ($d$) variable – and $Cp_{i_n, j_m}(d_{ref})$ is the *Cp* at the reference value for the parameter $d$ and for the given value of $i$ and $j$, the relevant normalized *Cp* value is given by:

$$Cpnorm_{i_n, j_m, d_t} = \frac{Cp_{i_n, j_m}(d_t)}{Cp_{i_n, j_m}(d_{ref})} \tag{8}$$

An overall number of 160 strings of *Cpnorm* – for the windward facades (a similar number for the leeward side) – were obtained and an equivalent number of strings of coefficients for the curve-fitting were calculated by the regression analysis.

Polynomial functions of various degrees were used in most of the curve-fitting (see Appendix). For the windward side, first- to third-degree polynomials were used. For the leeward side, first- to fifth-degree polynomials were used. The general equation in the case, for example, of a third-degree polynomial is:

$$Cpnorm_{i,j}(d) = a_0 + a_1(d)^1 + a_2(d)^2 + a_3(d)^3 \tag{9}$$

where, the variation range of $i$, $j$, and $d$ is the one of the specific parameter (see Section 4).

Non-polynomial functions were used for the parameters *far* and *sar* for which the fitting equation, in the case of windward facades, is shown in Section 4.3.

All curves were fitted using a very high correlation factor, generally 0.98–0.99 and never less than 0.95. As a feedback check for the windward side, the standard deviation *Sd* from measured *Cp* values corresponding to randomly selected values of the parameters for data calculated using the developed model was obtained by:

$$Sd = \frac{1}{N-1}\left\{\sum_{1}^{N}\left(\frac{|y_{cal} - y_{ref}|}{y_{ref}}\right)^2\right\}^{1/2} \tag{10}$$

where $y_{cal}$ and $y_{ref}$ are, respectively, the calculated and the reference *Cp* values.

Three sample data sets related to the parameters *pad*, *rbh*, *anw* and *xl* from both the reference tests were chosen. *Sd* was found ranging from 0.013 to 0.044 corresponding to a balanced average value of 0.024. These values confirm the correlation factors assumed for fitting.

Further tests are foreseen to check the interpolation of more data points and to compare the output of the model to other wind tunnel data sets performed in conditions similar to the reference tests.

### *3.3.2. Algorithm*

An algorithm was developed to calculate the *Cp* value for a generic given location on a wall of a block-shaped building and for given values of the considered parameters. It comprises the following steps:

(a) Calculation of a reference *Cp* at the given *zh* by using eqn. (7) with coefficients for Hussein and Lee's profiles (windward and leeward).

(b) Calculation of a *Cp* correction factor for each of the groups of parameters considered in the regression analysis. The correction factor is calculated using the curve-fitting equations for given values of the parameters. From eqns. (8) and (9):

$$Cf_{i_n, j_m, d_t} = Cpnorm_{i_n, j_m, d_t} = Cpnorm_{i_n, j_m}(d_t) \tag{11}$$

If $n$ and $m$ are equal to values considered in the regression analysis, the coefficients of the relevant fitting equations can be used to calculate the correction factor. If $n$ and $m$ are different from those

values, the correction factor is calculated for the closest lower and higher values and the two results linearly interpolated. An application range for each parameter is given according to the data scope within which the fitting process was performed.

(c) Multiplication of all the correction factors for the reference $Cp$ value in order to obtain the actual $Cp$ at the given context conditions. If $Cp_k$ is the surface pressure coefficient of the element $k$, with coordinates $xl$ and $zh$, on a facade of a building whose shape is defined by specific values of *far* and *sar*, and in climate-environmental conditions defined by specific values of $\alpha$, *pad*, *rbh*, and *anw*:

$$Cp_k = Cp_{ref}(zh) \times CF \tag{12}$$

where $CF$ is the global correction factor including the specific correction factors ($Cf$) related to each group of parameters:

$$CF = Cf_{zh}(\alpha) \times Cf_{zh}(pad) \times Cf_{zh,\,pad}(rbh) \times Cf_{zh,\,pad}(far) \times Cf_{zh,\,pad}(sar) \times Cf_{zh,\,anw}(xl) \tag{13}$$

### 3.3.3. *Cp calculation model*

The $Cp$ calculation program was written in standard Fortran 77 as a module of the COMIS multizone infiltration model. The program uses the algorithm described above (Section 3.3.2) and can be schematically divided into the following main parts, as shown in the flowchart of Fig. 6:

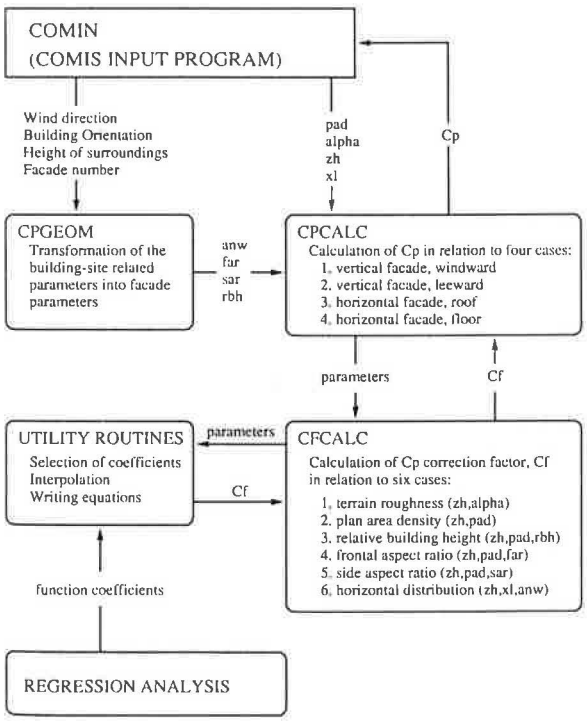


Fig. 6. Flowchart of the $Cp$ calculation progam.

(a) handling of geometrical input data related to environment and building;
(b) calculation of $Cp$;
(c) calculation of the $Cp$ correction factors;
(d) utility routines

In part (a), a routine transforms input data as described in the COMIS input program into parameters to be used by the $Cp$ calculation routines. The routine calculates *far*, *sar*, *rbh*, and *anw* in relation to building-site-related input parameters, namely, building outside dimensions, azimuth of the building and wind direction (both measured from the geographic north) [28].

In part (b), a routine calculates the reference $Cp$ value for the vertical position of the considered facade element and multiplies this value for the correction factors calculated in part (c).

In part (c), subroutines calculate the $Cp$ correction factors in relation to the six groups of parameters considered in the regression analysis (Sections 3.3.1, 3.3.2). The procedure deals with the windward as well as the leeward vertical facades and is written in such a way that allows for adding the calculation of the surface pressure distribution on roof and floor as soon as the relevant fitting data are available.

In part (d), specific subroutines are used to search the proper coefficient for the fitting equations and to interpolate if necessary.

This modular framework allows for adding or changing reference input data by simply operating on the fitting function coefficients and/or adding new parameters developing the relevant specific routines.

The application limits of the model are related to the variation range defined for each parameter. In particular, the model cannot be applied to:

- high terrain roughness ($\alpha > 0.33$) and/or high density of the immediate surrounding buildings ($pad > 50$);
- immediate surrounding buildings with staggered or irregular pattern layout;
- immediate surrounding buildings with $pad > 12.5$, when the considered building has different height from its surroundings or different shape from a cube;
- buildings 4 times higher or 0.5 lower than the surroundings;
- buildings with irregular shape or overhangs;
- regular block-shaped buildings with aspect ratios less than 0.5 or greater than 4.

Output data of the model are single $Cp$ values, each related to a specific two-dimensional position of a surface element on the wall, and to wind direction, as well as arrays of $Cp$ values, at regular intervals, for locations and wind directions.

## 4. Analysis

The following is a description of the regression analysis carried out for each of the groups of parameters described above on data related to the windward side. An analogous process was used to characterize the data related to the leeward side. Equations and coefficients for the curve-fitting are shown in the Appendix.

### *4.1. Effect of terrain roughness*

The effect of terrain roughness on wind pressure distribution was evaluated by analyzing the variation of *Cp* with velocity profile exponent along the vertical centreline of the cube-shaped model of the two tests with normal approach wind.

First, the theoretical curves corresponding to the $\alpha$ values disclosed in the reference tests were compared to new curves drawn by fitting the measured mean wind speed data included in the reports. As shown in Fig. 7, both tests reveal an under-evaluation of the mean wind velocity except in the case of free stream [22].

This discrepancy is due to the inaccuracy of the power law equation as pointed out by some authors [8, 11] who prefer the applications of a logarithmic regression (see Section 1). It is practically impossible to fit with high accuracy the entire wind velocity profile, i.e., for the whole thickness of the boundary layer, by using the power law equation. In the case of Hussein and Lee's test, for example, $\alpha = 0.28$ fits relatively well to the upper half of the profile while $\alpha = 0.22$ fits similarly well to the upper one-fourth of the profile and much better to the lower one-fourth of the profile.

Several attempts were made to fit the data using all the $\alpha$ values shown in Fig. 7. Three values for $\alpha$ were eventually selected: 0.10, for Akins and Cermak's data related to smooth terrain; 0.22, for Hussein and Lee's data; and 0.31, for averaged data between the two roughest of Akins and Cermak's boundary layers corresponding to $\alpha = 0.34$ and $\alpha = 0.38$. The latter Akins and Cermak's profiles are so close to each other that no significant effect was found on the relevant sets of *Cp* data (see Fig. 7). All data are related to a cube-shaped model. The *Cp* data were converted with respect to the selected values of $\alpha$ using eqn. (6). The three *Cp* profiles are shown in Fig. 8.

The *Cp* data corresponding to the three values of $\alpha$ were then normalized with respect to *Cp* at $\alpha = 0.22$ for each of the chosen values of *zh* (0.1, 0.3, 0.5, 0.7, 0.9). Second-degree polynomials were used for the relevant curve-fitting (Fig. 9). The limits

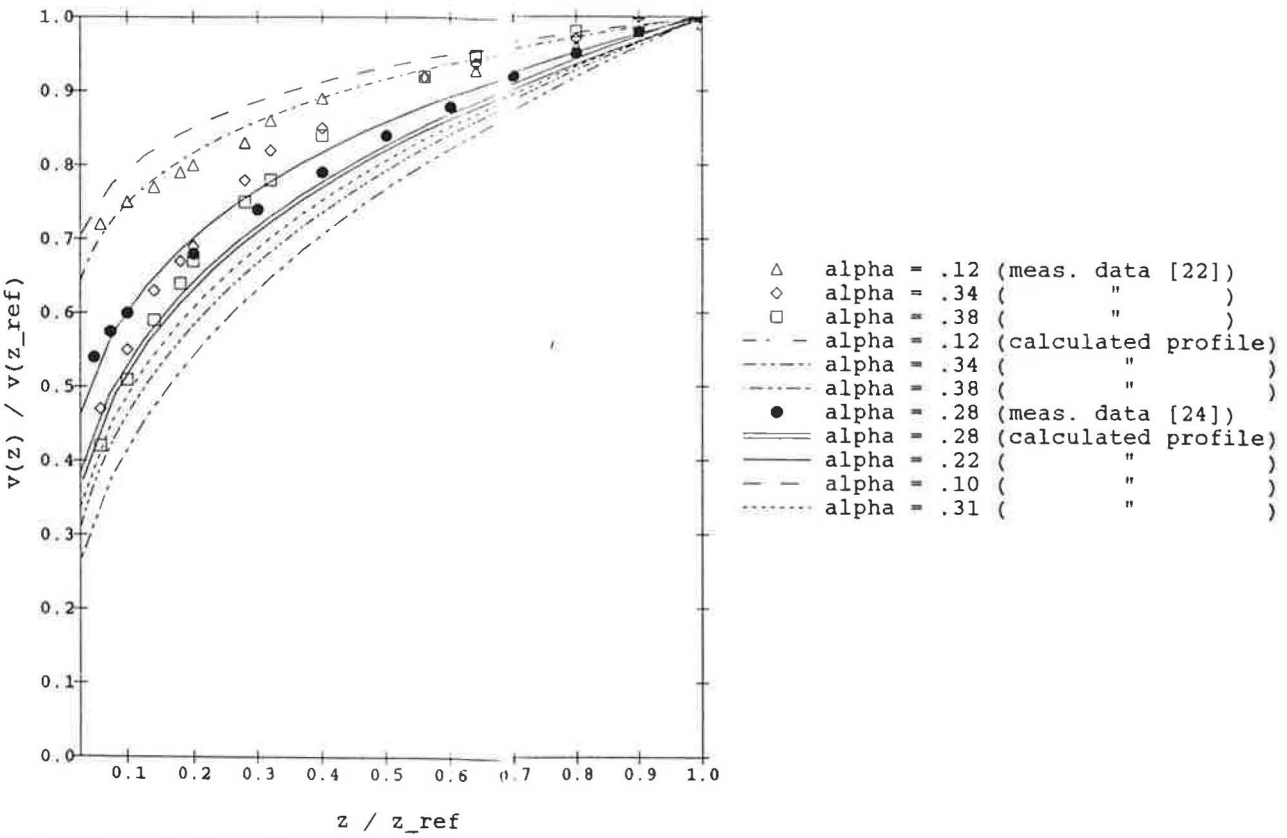


Fig. 7. Wind velocity profiles — $z_{ref}$: upstream.

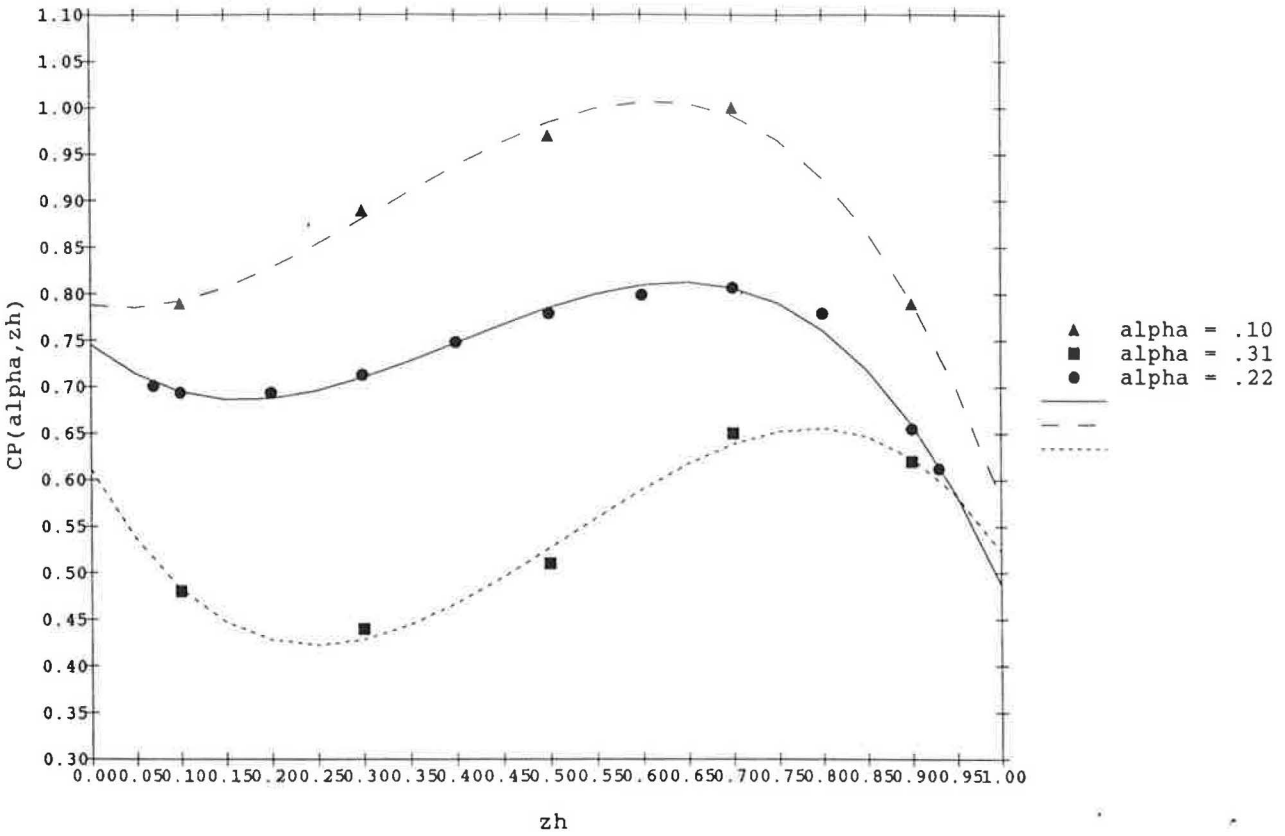


Fig. 8. *Cp* cube centreline vertical profiles at various $\alpha$.

given for the variation range of $\alpha$ in the calculation model are $0.10 \leqslant \alpha \leqslant 0.33$.

As the graph shows, the normalized *Cp* generally decreases with increasing of $\alpha$. Its variation rate, i.e., the *Cp* standard deviation represented by the tip of the curves, decreases with increasing of *zh*. Exception to the latter trend occurs at the bottom of the profile ($zh = 0.1$). The smoothest variation trend is shown at $zh = 0.7$ where the curve is close to a straight line.

### 4.2. *Effect of surrounding buildings*

The following parameters from Hussein and Lee's tests were used to analyse the effect of surrounding buildings on *Cp* distribution:

- plan area density (*pad*)
- relative building height (*rbh*)

Plan area density is defined as ratio of built area to total area (Fig. 10). This ratio has to be calculated within a radius ranging from 10 to 25 times the height of the considered building — values corresponding to those the model group size required for the surface pressure forces to stabilize because of turbulence effects [24, pp. 15–17]. The normal layout pattern was taken into account in the present analysis amid the two considered by the authors (Section 3.2).

Relative building height is the ratio of the height of the considered building to the height of the surrounding buildings, the latter assumed to be regular blocks of the same height.

A *Cp* data set taken from cube-shaped model profiles and related to fourteen values of *pad* (0, 3.125, 5.0, 6.25, 7.5, 10.0, 12.5, 17.5, 20.0, 25.0, 30.0, 40.0, 50.0) for eleven values of *zh* (0.07, 0.1–0.9, 0.93) was analysed in order to model the variation of *Cp* with plan area density [25, p. 29].

*Cp* decreases with *pad* at any value of *zh* with differing variation rates. Three patterns occur corresponding to three flow regimes as defined according to a classification of the flow over roughness elements first introduced by Morris [29]. These flow regimes applicable to pipe flows, open channel flows and flat plate boundary layers are denoted as isolated roughness flow, wake interference flow and skimming flow regimes.

In the isolated roughness flow, the roughness elements are sufficiently far apart such that each element acts as if in isolation and behind which the wake and the separation bubble develop completely and reattachment occurs before the next element is reached. In the wake interference flow the roughness elements are close enough to each other so that the separation bubble associated with

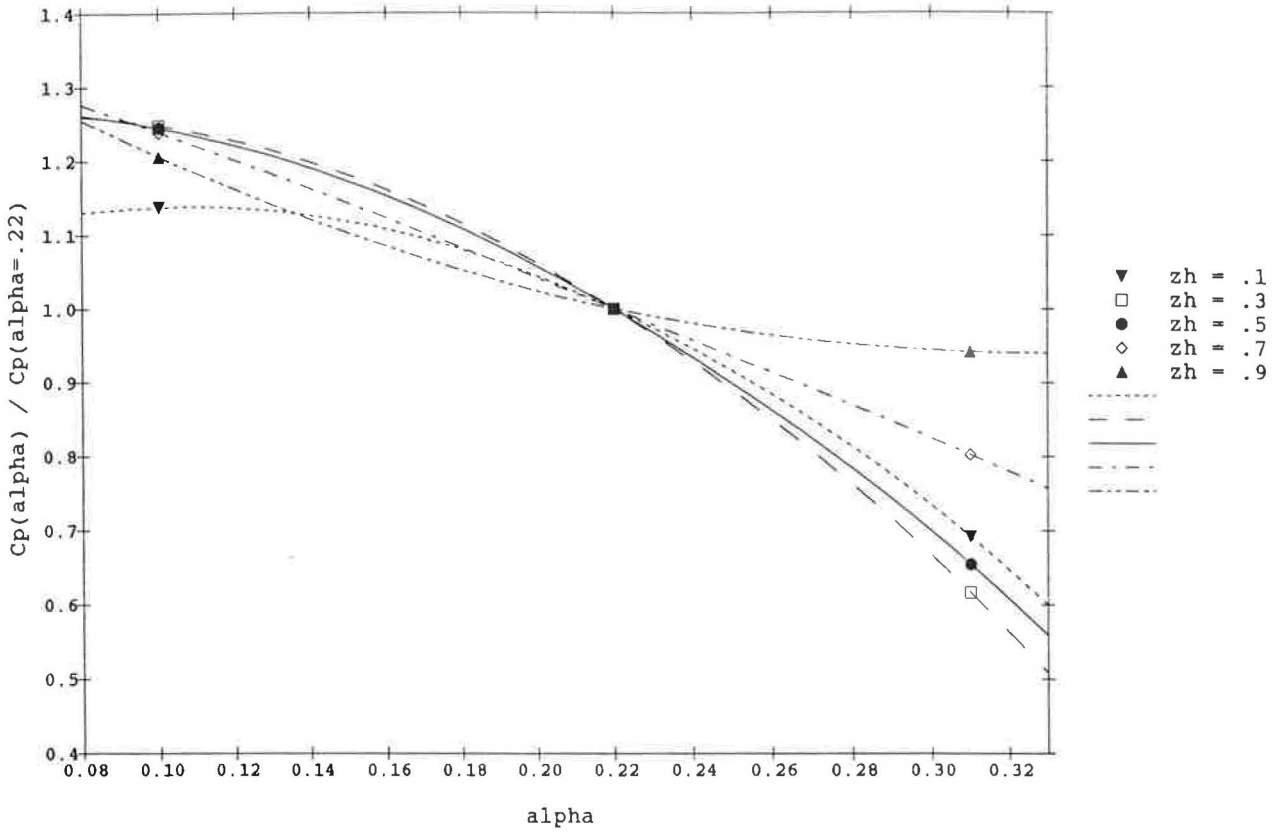


Fig. 9. $Cp_{zh}(\alpha)$ normalized with respect to $Cp_{zh}(\alpha = 0.22)$.

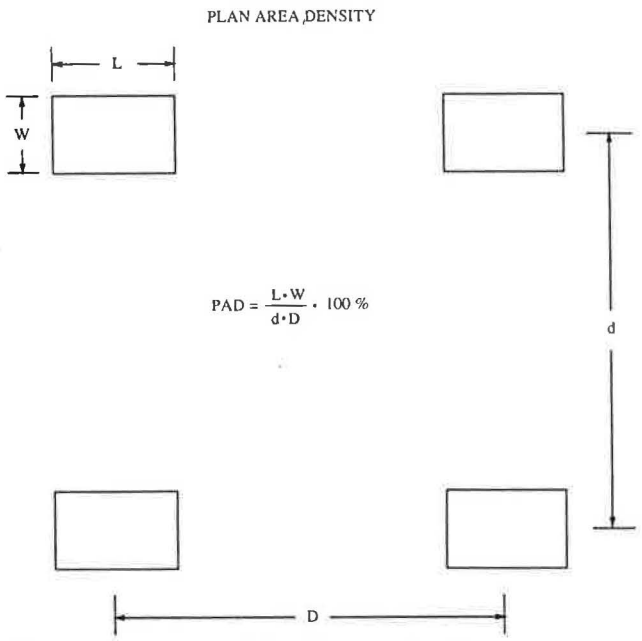


Fig. 10. Calculation of the plan area density.

each element does not have room to develop fully. In the skimming flow, the roughness elements are closer still so that the stable vortices are created in the space between the elements and the flow appears to skim on the crest of the elements. Hence the main effect of roughness geometry as characterized by its density is to change one flow regime to another. The first change, from an isolated roughness flow regime into a wake interference flow regime, occurs when changing *pad* from 10 to 12.5. The second change, from a wake interference to a skimming flow regime, is indicated by the initiation of a stable vortex between roughness elements at $pad = 17.5$ [25, pp. 9–12].

Four *Cp* data sets taken from models of different heights with respect to the roughness array of cubes – $rbh = 0.5, 0.8, 1.0, 1.3, 1.5, 2.0, 3.0, 4.0$ – and related to four values of *pad* (0, 5.5, 12.5, 25.0) for seven values of *zh* (0.07, 0.2, 0.5, 0.7, 0.8, 0.9, 0.93) were analysed in order to model the variation of *Cp* with relative building height [26, pp. 15–18]. When $pad = 0$, the reference model for *rbh* is the central cube [24, p. 36].

*Cp* increases with *rbh* at any given *pad*. Its variation rate increases with *zh* reaching a maximum roughly at $zh = 0.85$.

The *Cp* data from the *plan area density* set related to a cube-shaped model were normalized with respect to *Cp* at $pad = 0$ for each value of *zh*. Five third-degree polynomials were used for the curve-fitting of the normalized *Cp* data (Fig. 11).

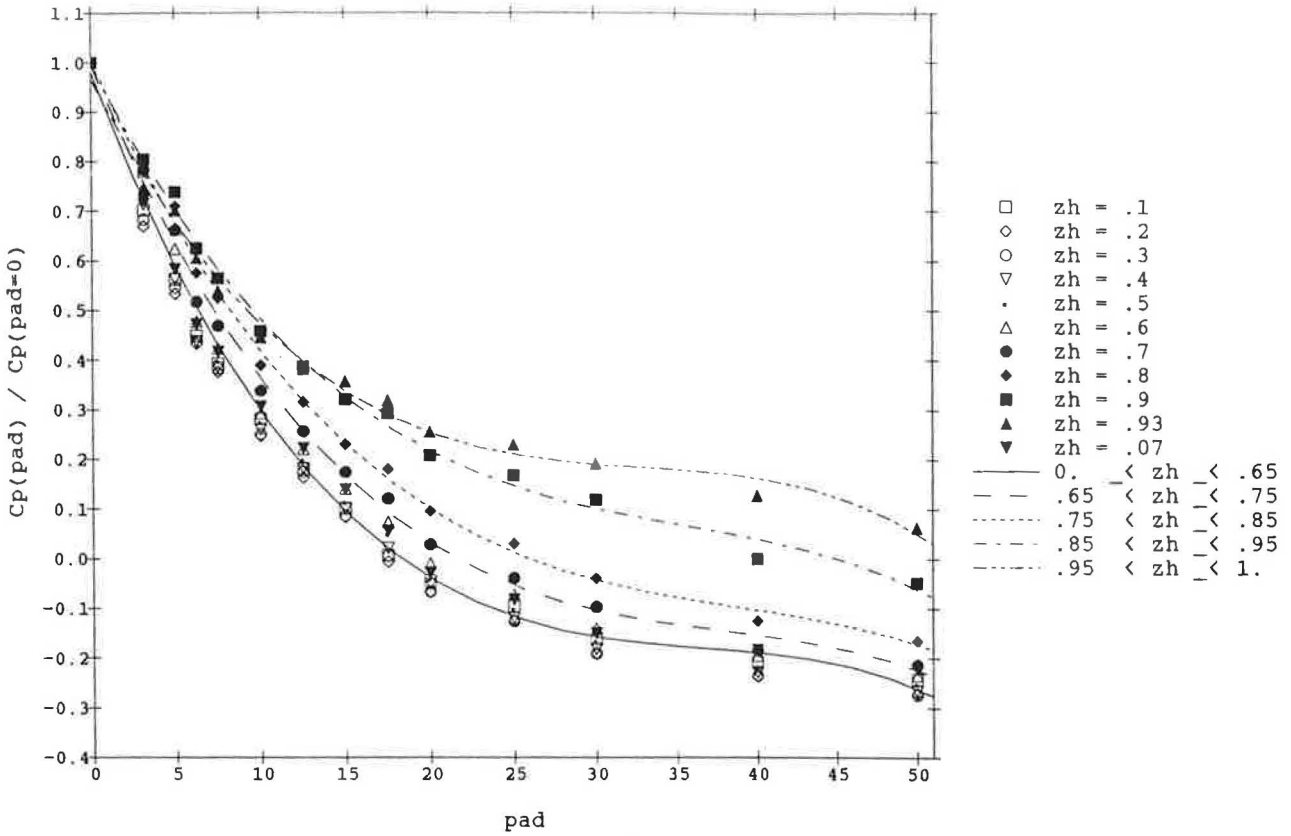


Fig. 11. $Cp_{zh}(pad)$ normalized with respect to $Cp_{zh}(pad=0)$.

The curves show a smooth concave shape reversing to convex shape at $pad \geqslant 40$ and a decreasing of concavity with height. The effect of the above-mentioned different flow regimes is apparent where the curve at $zh = 0.93$ overlaps the curve at $zh = 0.90$. It occurs at $pad \simeq 12$ corresponding to the change from an isolated roughness flow regime into a wake interference flow regime.

The *Cp* data from the four *relative building height* sets were normalized with respect to *Cp* at $rbh = 1$ (cube-shaped model) for each combination of *zh* and *pad*. Figure 12 shows the curve-fittings related to three values of *zh* as examples. The curve-fitting uses a straight line for all *zh* in the case of an isolated model. The curve-fitting for $pad = 5.5$, 12.5 uses a straight line for all *zh* except $zh = 0.90$ and $zh = 0.93$ for which second-degree polynomials are used. The curve-fitting for $pad = 25$ uses third-degree polynomials at $zh = 0.07$, 0.3, 0.5, 0.7, and, second-degree polynomials at $zh = 0.1$, 0.9, 0.93.

### 4.3. *Effect of aspect ratios*

Frontal and side aspect ratios were the parameters used to evaluate the influence of the model geometry on the *Cp* centreline vertical profile. In Hussein and Lee's tests, the frontal aspect ratio is the ratio of the length of the facades normal to the wind to the height of the model, the side aspect ratio is the ratio of the length of the facades parallel to the wind to the height of the model. In the calculation model, where more wind angles are considered, the frontal aspect ratio is related to the considered facade and the side aspect ratio to its adjacent facade whichever angle the wind direction forms with the facades themselves.

*Cp* decreases with increase of *far* at any *zh* on an isolated model when $far \geqslant 1$. To the contrary, *Cp* is greater on the model with $far = 0.5$ than on the other models above $zh \simeq 0.75$. The side aspect ratio has little influence on the variation of *Cp* [24, p. 41].

When an array of models is considered ($pad \neq 0$), the centreline *Cp* on the windward facade of the central model generally increases with *far* and *sar* for any given *pad* and *zh*. The increase is higher at lower values of the aspect ratios [25, pp. 52–55 and 64–66]. Conversely, *Cp* decreases with *pad* at a given *far* or *sar* as it occurs on a cube-shaped model.

*Cp* was normalized with respect to the *Cp* on the cube-shaped model ($far = 1$, $sar = 1$) for each combination of the chosen values of *zh* (0.07, 0.2, 0.4, 0.6, 0.8, 0.93) and *pad* (0, 5, 7.5, 10, 12.5).

The curve-fitting uses a straight line for $far < 1$ and $sar < 1$. For $far > 1$ and $sar > 1$, the function used is:

$$Cpnorm_{pad,\,zh}(d) = \left\{ a_1 d + \frac{a_2}{d} + a_3 \right\}^{1/2} \qquad (14)$$

where $d = far$ or $sar$, $0.5 \leqslant far \leqslant 4.0$, and $0.5 \leqslant sar \leqslant 2.0$.

Figures 13 and 14 show examples of these curves ($far > 1$, $sar > 1$).

*4.4. Effect of wind direction*

The analysis to determine the effect of wind direction on *Cp* distribution was carried out by using data sets from Akins and Cermak's test [22] related to a square-plan model with height and velocity profile exponent averaged among several values (Section 2.2.2).

First, *Cp* related to the vertical centreline of a facade were normalized with respect to the *Cp* at $anw = 0°$ for ten values of *zh* (Fig. 15).

Second-degree polynomials were used for the curve-fitting and three functions — corresponding to *zh* 0.5, 0.7, 0.9 — were able to represent the entire range of the relative vertical positions.

As the second step, the effect of wind direction on the *Cp* horizontal distribution was evaluated

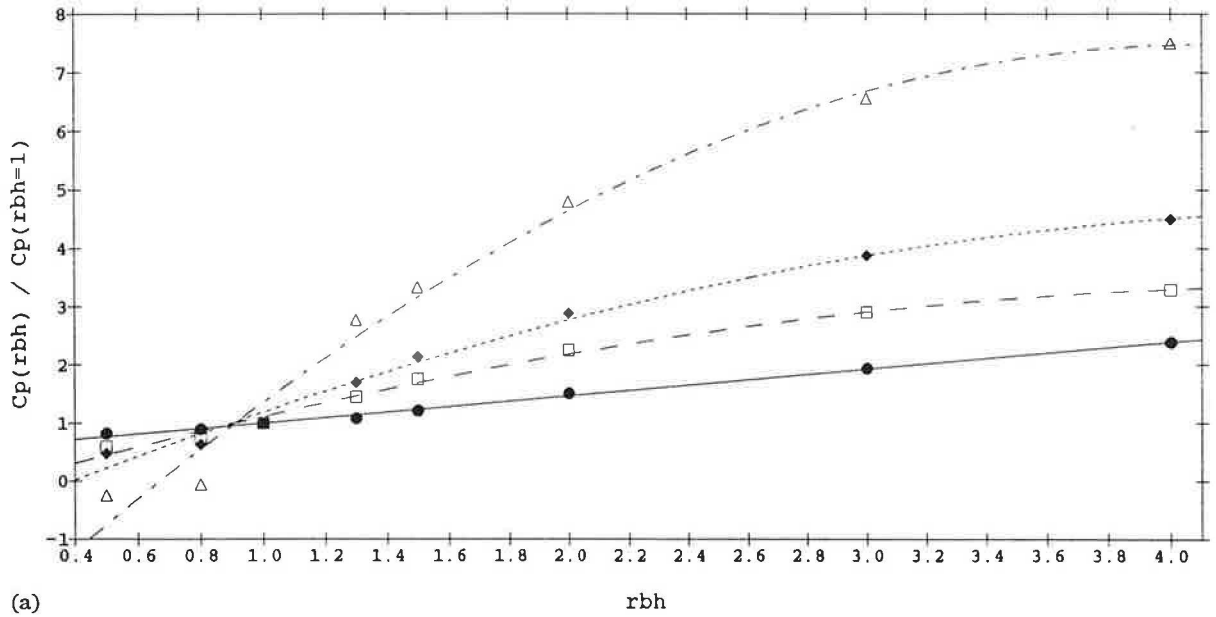


(a)

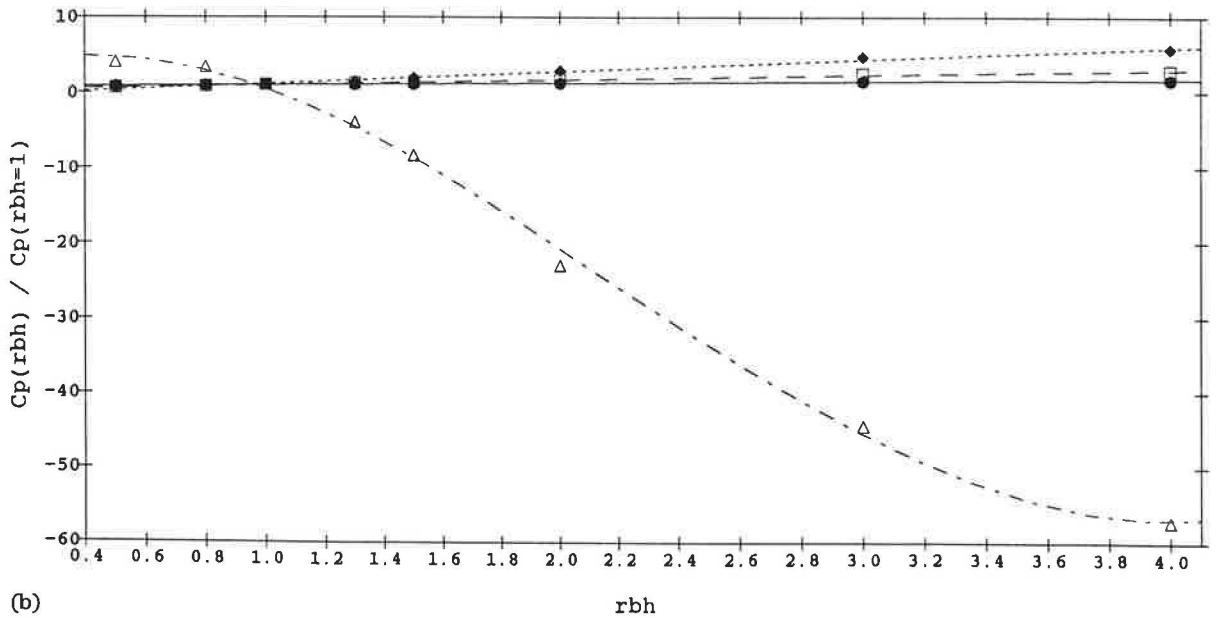


(b)

Fig. 12.

*(continued)*

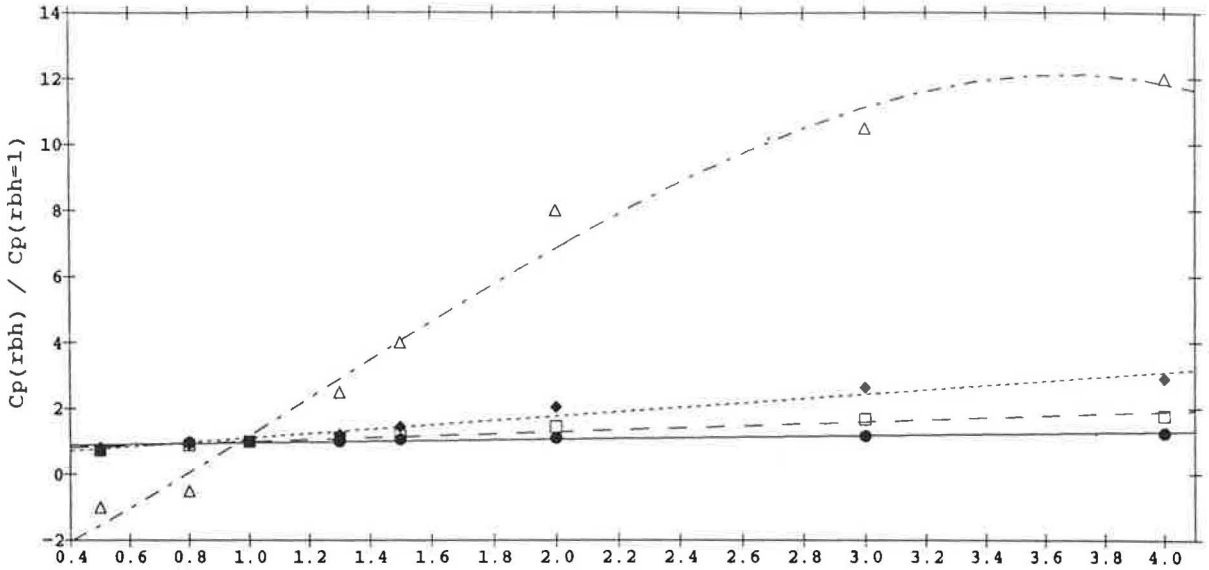


(c)

Fig. 12. $Cp_{zh,pad}(rbh)$ normalized with respect to $Cp_{zh,pad}(rbh=1)$. ● $pad=0$; □ $pad=5.5$; ◆ $pad=12.5$; △ $pad=25.0$: (a) $zh=0.93$; (b) $zh=0.5$; (c) $zh=0.07$.

using the parameters *anw*, *xl*, and *zh*. The *Cp* data sets were represented in relation to their location coordinates on each facade of the model, *xl* and *zh*, determined as shown in Fig. 16.

The wind incidence angle, *anw*, was defined as the angle that the approaching wind forms with the normal to each facade as described in Fig. 17. *Cp* data corresponding to nine values of *anw* – 0, 20, 40, 70, 90, 110, 140, 160, 180° – for eleven values of *xl* (0.0–1.0) were taken from Akins and Cermak's report. Extrapolated *Cp* data by curve-fitting were used for *anw* = 10, 30, 50, 60, 80, 100, 120, 130, 150, 170° in order to obtain a regular 10° interval. A *Cp* value is considered on the windward side if $0° \leqslant anw < 90°$, on the leeward side if $90° \leqslant anw \leqslant 180°$. Only absolute values of *anw* were used for the regression analysis. The *Cp* value for $anw = \phi$ at a given location (*zh*, *xl*) is equal to the *Cp* value for $anw = -\phi$ at location (*zh*, $1 - xl$).

*Cp* was normalized with respect to *Cp* at $xl = 0.5$ in relation to the three selected values of *zh* for each of the nineteen values of *anw*. The windward side *Cp* data were fitted using 2nd-degree polynomials. A 3rd-degree polynomial was used for *anw* 90°. In Fig. 18 one of the three plots is shown as example.

These normalized *Cp* were used to calculate the correction factor related to the wind incidence angle and to the horizontal coordinate of a surface element.

## 5. Conclusions

The work performed shows that it is possible to calculate the combined effect of environmental and geometrical conditions on the wind pressure distribution around buildings with sufficient accuracy. The degree of accuracy is proportional to the availability of data from wind tunnel or real-scale tests for the regression analysis upon which the developed model is based.

It is also shown that *Cp* values can be calculated at *any* position of a building facade and for *any* values of the considered parameters within limits depending only on the characteristics of the reference data used for the regression analysis. This procedure, developed by using a parametrical approach and a simple algorithm, allows *Cp* values to be obtained without having to match pre-defined environmental and geometrical conditions.

Perhaps the most useful contribution of this work is the methodology developed rather than the specific results of the analysis, e.g., fitting equations and relevant coefficients. The discovery of lack of data led to the defining of a framework for future work.

### *5.1. Future work*

Analysis has revealed the main problem as being a lack of reference data sets as well as homogeneous experimental settings consistent with the characteristics of a parametrical approach. The correction made to the values of the wind velocity profile exponent and the limitation imposed on the application range of other parameters, namely, relative building height and aspect ratios, are some of the consequences of that situation.

The most effective and thorough way to overcome these problems would be to perform a whole set

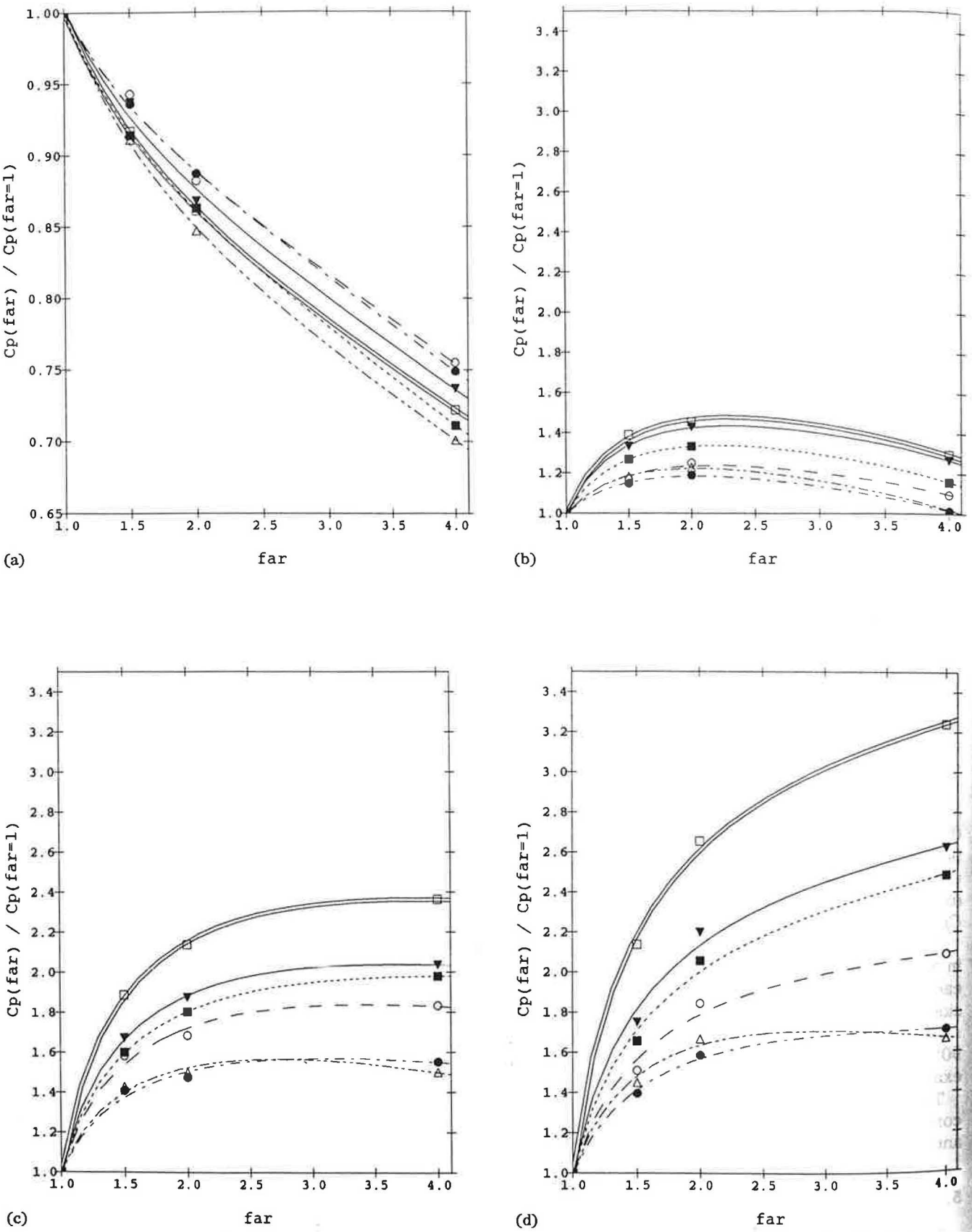


Fig. 13. $Cp_{zh,\,pad}(far)$ normalized with respect to $Cp_{zh,\,pad}(far=1)$. ▼ $zh=0.07$; □ $zh=0.2$; ■ $zh=0.4$; ○ $zh=0.6$; ● $zh=0.8$; △ $zh=0.93$. (a) $pad=0$; (b) $pad=5$; (c) $pad=10$; (d) $pad=12.5$.

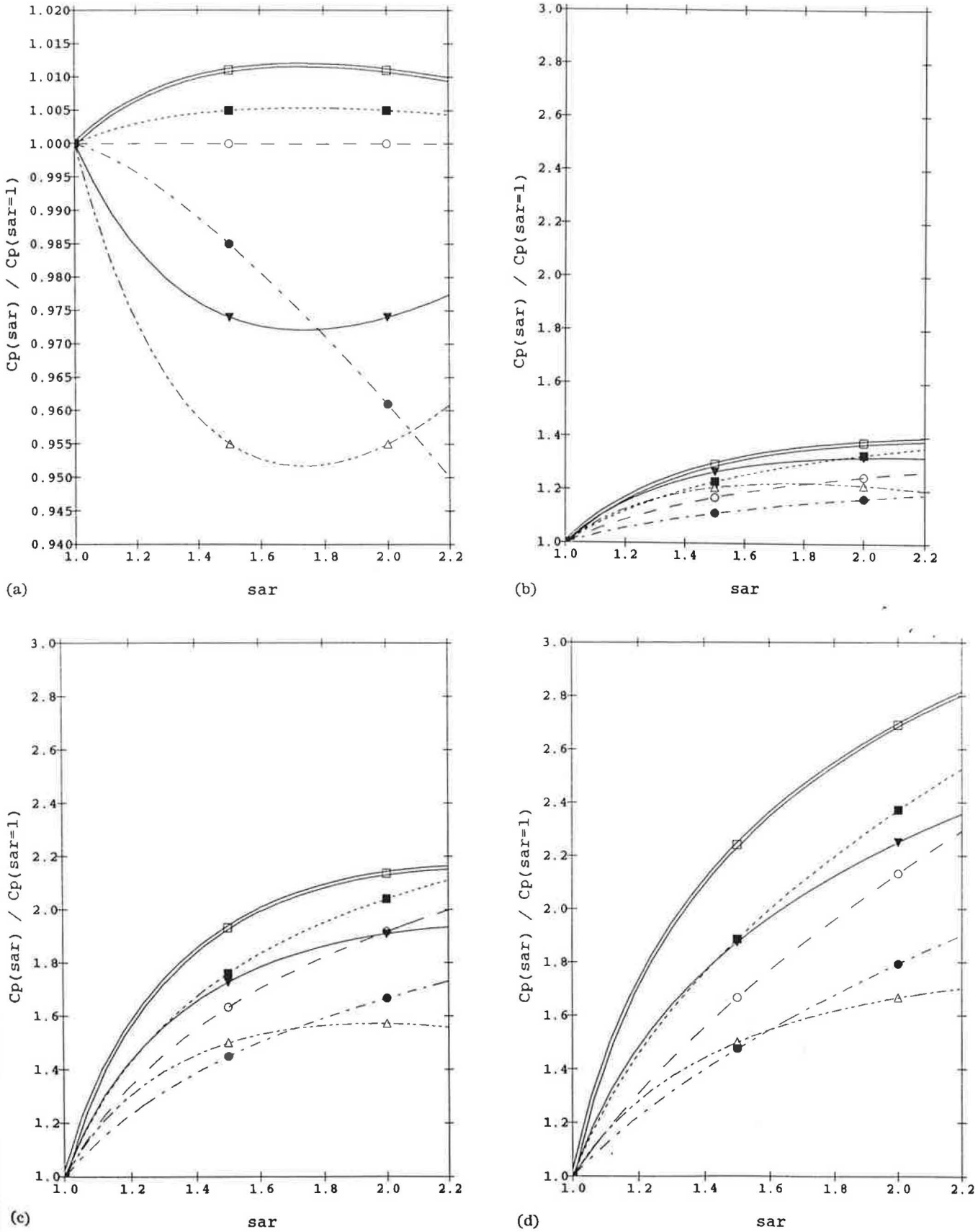


Fig. 14. $Cp_{zh,\,pad}(sar)$ normalized with respect to $Cp_{zh,\,pad}(sar=1)$. ▼ $zh=0.07$; □ $zh=0.2$; ■ $zh=0.4$; ○ $zh=0.6$; ● $zh=0.8$; △ $zh=0.93$; (a) $pad=0$; (b) $pad=5$; (c) $pad=10$; (d) $pad=12.5$.

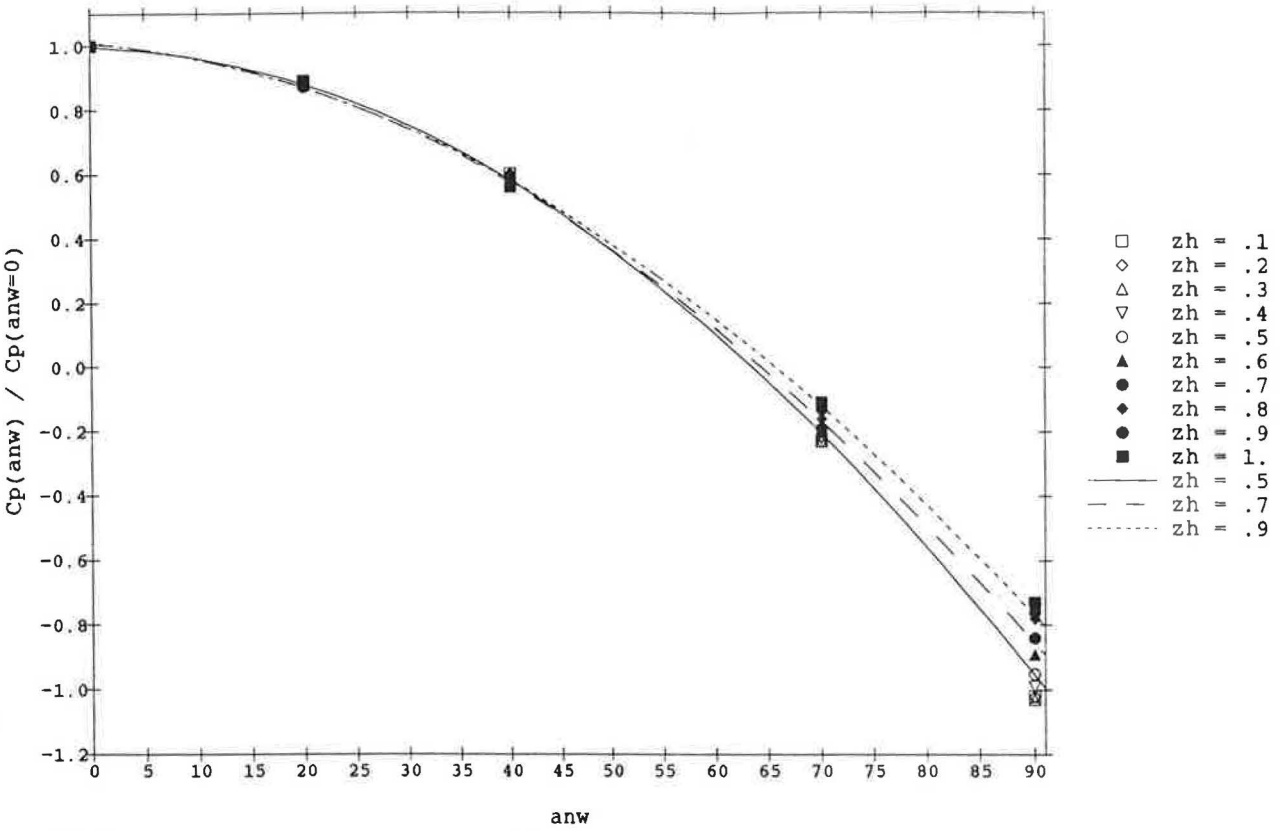


Fig. 15. $Cp_{zh,xl=0.5}(anw)$ normalized with respect to $Cp_{zh,xl=0.5}(anw = 0°)$.

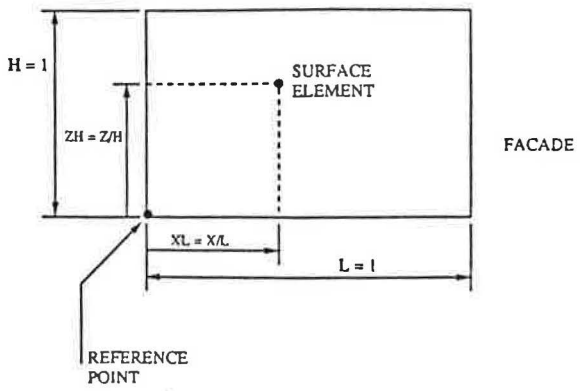


Fig. 16. Facade element positioning.

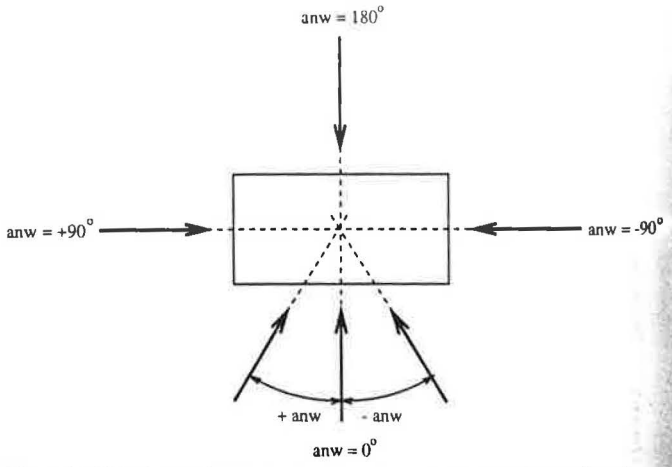


Fig. 17. Wind incidence angle in relation to the front facade — plan view.

of wind tunnel tests *ad hoc* for the development of a calculation model as the one described here. It would be a cumbersome and time-consuming task which could be only partially carried out within the framework of the recently started IEA-ANNEX 23 on multizone infiltration modelling.

## Nomenclature

| | |
|---|---|
| $a_{1...n}$ | coefficients for the curve-fitting equations (–) |
| *anw* | wind incident angle, measured from the normal to each wall (–) |
| *d* | zero flow plane displacement height in the wind velocity profile logarithmic equation (m) |
| *far* | frontal aspect ratio, ratio of model length to model height (–) |
| *g* | acceleration of gravity (m/s$^2$) |
| *h* | eave height of a building/model (m) |

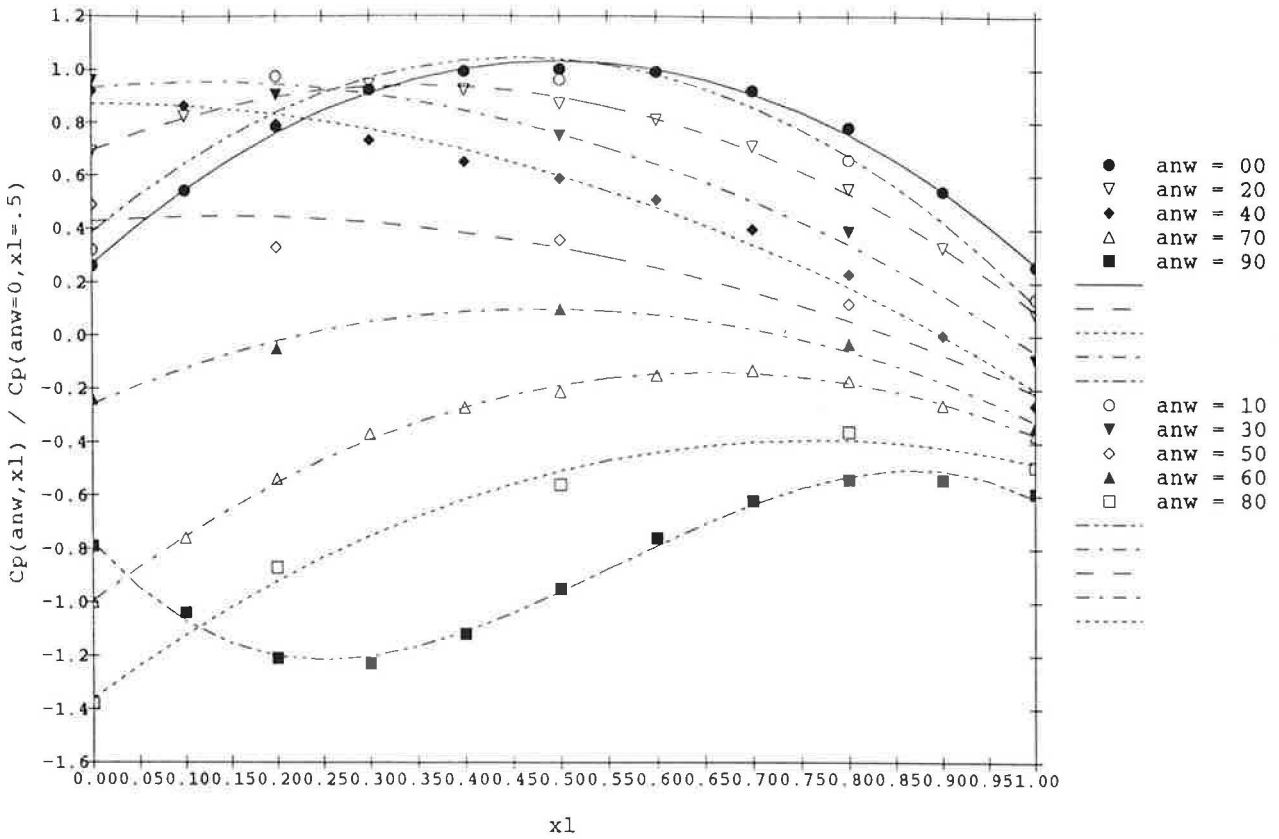


Fig. 18. $Cp_{zh,anw}(xl)$ normalized with respect to $Cp_{zh,anw}(xl=0.5)$.

| | |
|---|---|
| $k$ | surface element on building/model facade (–) |
| *pad* | plan area density, representing the density of surrounding buildings (–) |
| *rbh* | relative building height, ratio of model height to height of surroundings (–) |
| *sar* | side aspect ratio, ratio of model width to model height (–) |
| $v$ | air velocity (m/s) |
| *xl* | ratio of the position of a facade element to the length of the facade (–) |
| $z_0$ | roughness length in the wind velocity profile logarithmic equation (m) |
| $z_{ref}$ | reference height for wind velocity measurements (m) |
| $z$ | height above ground (m) |
| *zh* | ratio of the position of a facade element to the height of the facade (–) |
| *Cf* | *Cp* correction factor for a specific parameter (–) |
| *Cp* | surface pressure coefficient (–) |
| $Cp_{ref}$ | reference surface pressure coefficient (–) |
| *Cpnorm* | normalized surface pressure coefficient (–) |
| *CF* | global *Cp* correction factor (–) |
| *N* | number of measurement or calculated points (–) |
| $P_0$ | atmospheric pressure (Pa) |
| $P_{dym}$ | dynamic pressure (Pa) |
| $P_k$ | total pressure at surface element $k$ (Pa) |
| $P_{stat}$ | static pressure (Pa) |
| *Sd* | standard deviation (–) |
| *wpd* | wind pressure distribution |
| $\alpha$ | wind velocity profile exponent, characteristic of the roughness (–) |
| $\rho$ | air density (kg/m$^3$) |
| $\rho_{out}$ | density of the outside air (kg/m$^3$) |

## References


1 *Characteristics of Wind Speed in the Lower Layers of the Atmosphere near the Ground: Strong Winds (Neutral Atmosphere)*, *ESDU Data Item No 72026*, Engineering Sciences Data Unit, London, 1972.

2 *Characteristics of Atmospheric Turbulence near the Ground, ESDU Data Items Nos. 74030, 74031, 75001*, Engineering Sciences Data Unit, London, 1975.

3 R. M. Aynsley, W. Melbourne and B. J. Vickery, Wind tunnel testing techniques, *Architectural Aerodynamics*, Applied Science Publishers Ltd., London, 1977, p. 163.

4 O. G. Sutton, The logarithmic law of wind structure near the ground, *Q. J. Roy. Meteorol. Soc.*, *62* (1936) 124–127, *63* (1937) 105–107.

5 D. Brunt, *Physical and Dynamical Meteorology*, Cambridge University Press, Cambridge, 2nd edn., 1952, p. 114.

6 A. G. Davenport, *Wind Loads on Structures, Technical Paper No. 88*, National Research Council, Division of Building Research, Ottawa, Canada, March, 1960.

7 A. G. Davenport, The interaction of wind and structure, in E. J. Plate (ed.), *Engineering Meteorology*, Elsevier, Amsterdam, 1982.

8 M. Jensen, The model law for phenomena in the natural wind, *Ingeniøren–Int. Edn.*, *2* (4) (Nov.) (1958).

9 V. B. Torrance, Wind profiles over a suburban site and wind effects on a half full-scale model building, *Build. Sci.*, *7* (1972) 1–12.

10 N. J. Cook, Wind-tunnel simulation of the adiabatic atmospheric boundary layer by roughness, barrier and mixing-device methods, *J. Indust. Aerodyn.*, *3* (1978) 157–176.

11 N. J. Cook, *The Designer's Guide to Wind Loading of Building Structures*, Building Research Establishment Report, Butterworths, 1985.

12 Air flow around buildings, *ASHRAE Handbook of Fundamentals 1989*, ASHRAE, SI Edn., Ch. 14.3.

13 A. G. Davenport, A rationale for the determination of the basic design wind velocities, *ASCE-Proc.*, *'86*, 1960, pp. 36–38 (from ref. 16).

14 M. W. Liddament, *Air Infiltration Calculation Techniques – an Applications Guide*, AIC–AG–I–86, Air Infiltration and Ventilation Centre, Bracknell, UK, 1986.

15 B. G. Wiren, *Effects of Surrounding Buildings on Wind Pressure Distributions and Ventilation Losses for Single-Family Houses, Bulletin M85:19*, National Swedish Institute for Building Research, Gavle, Sweden, Dec., 1985.

16 H. G. Kula and H. E. Feustel, *Review of Wind Pressure Distribution as Input Data for Infiltration Models, Report LBL–23886*, Lawrence Berkeley Laboratory, Berkeley, CA, 1988.

17 *Proc. Tech. Note AIC 13.1*, Air Infiltration and Ventilation Centre, Bracknell, U.K., Nov., 1984.

18 C. Allen, *Wind Pressure Data Requirements for Air Infiltration Calculations, Tech. Note AIC 13*, Air Infiltration and Ventilation Centre, Bracknell, UK, Jan., 1984.

19 K. Bala'zs, Effect of some architectural and environmental factors on air filtration of multistorey buildings, *Proc. 3rd ICBEM, Vol. III*, Lausanne, Switzerland, 1987, pp. 21–28.

20 M. V. Swami and S. Chandra, *Procedures for Calculating Natural Ventilation Airflow Rates in Buildings, Final Report FSEC-CR-163-86*, Florida Solar Energy Center, Cape Canaveral, FL, March, 1987.

21 M. Hussein and B. E. Lee, *An Investigation of Wind Forces on Three Dimensional Roughness Elements in a Simulated Atmospheric Boundary Layer, BS 55*, Department of Building Science, University of Sheffield, UK, July, 1980.

22 R. E. Akins and J. E. Cermak, *Wind Pressures on Buildings, CER76-77REA-JEC15*, Fluid Dynamic and Diffusion Laboratory, Colorado State University, CO, 1976.

23 A. J. Bowen, *A Wind Tunnel Investigation using Simple Building Models to obtain Mean Surface Wind Pressure Coefficients for Air Infiltration Estimates, Lab. Tech. Report, LTR-LA-209*, National Aeronautical Establishment, Ottawa, Canada, Dec., 1976.

24 M. Hussein and B. E. Lee, *An Investigation of Wind Forces on Three Dimensional Roughness Elements in a Simulated Atmospheric Boundary Layer, BS 55, Part I, Flow Over Isolated Roughness elements and the Influence of Upstream Fetch*, Department of Building Science, University of Sheffield, UK, July, 1980.

25 M. Hussein and B. E. Lee, *An Investigation of Wind Forces on Three Dimensional Roughness Elements in a Simulated Atmospheric Boundary Layer, BS 56, Part II, Flow over Large Arrays of Identical Roughness Elements and the Effect of Frontal and Side Aspect Ratio Variations*, Department of Building Science, University of Sheffield, UK, July, 1980.

26 M. Hussein and B. E. Lee, *An Investigation of Wind Forces on Three Dimensional Roughness Elements in a Simulated Atmospheric Boundary Layer, BS 57, Part III, The Effect of Central Model Height Variations Relative to the Surrounding Roughness Arrays*, Department of Building Science, University of Sheffield, UK, July, 1980.

27 *RS/1, Release 4*, BBN Software Products Corporation, Cambridge, MA, Copyright 1988.

28 H. E. Feustel *et al.*, *COMIS – User Guide, 5.6.3., Cp-Calculation Routines*, Air Infiltration and Ventilation Centre, Bracknell, U.K., 1991, to be published.

29 H. M. Morris, Jr., Flow in rough conduits, *Trans. ASCE*, *120* (1955) Paper No. 2745 (from ref. 24).


## Appendix

*Coefficients for the curve-fitting equations – Windward side*

Polynomial function for the reference *Cp* (eqn. (7)):

$$CP_{ref}(zh) = -2.381082zh^3 + 2.89756zh^2 - 0.774649zh + 0.745543$$

Coefficients for the equations of the normalized *Cp* as a function of environmental and geometrical parameters as follows:

Coefficients for the equations of the normalized *Cp* as a function of terrain roughness: $Cpnorm_{zh}(\alpha) = a_0 + a_1(\alpha) + a_2(\alpha)^2$

| $zh$ | $a_2$ | $a_1$ | $a_0$ |
|---|---|---|---|
| 0.1 | −10.820106 | +2.312434 | +1.014958 |
| 0.3 | −10.42328 | +1.268783 | +1.225354 |
| 0.5 | −8.531746 | +0.688492 | +1.261468 |
| 0.7 | −0.939153 | −1.691138 | +1.417505 |
| 0.9 | 5.10582 | −3.350529 | +1.489995 |

Coefficients for the equations of the normalized $Cp$ as a function of density of surrounding buildings: $Cpnorm_{zh}(pad) = a_0 + a_1(pad) + a_2(pad)^2 + a_3(pad)^3$

| $zh$ | $a_3$ | $a_2$ | $a_1$ | $a_0$ |
|---|---|---|---|---|
| 0.0 → 0.65 | −2.14966e-05 | +2.37444e-03 | −0.089797 | +0.979603 |
| 0.66 → 0.75 | −1.775637e-05 | +2.034996e-03 | −0.081741 | +0.995399 |
| 0.76 → 0.85 | −1.523628e-05 | +1.788998e-03 | −0.074881 | +1.00378 |
| 0.86 → 0.95 | −1.571837e-05 | +1.693211e-03 | −0.06647 | +0.994355 |
| 0.96 → 1.0 | −1.987115e-05 | +1.968606e-03 | −0.067063 | +0.966038 |

Coefficients for the equations of the normalized $Cp$ as a function of height of surrounding buildings: $Cpnorm_{zh,\,pad}(rbh) = a_0 + a_1(rbh) + a_2(rbh)^2 + a_3(rbh)^3$

| $zh$ | $pad$ | $a_3$ | $a_2$ | $a_1$ | $a_0$ |
|---|---|---|---|---|---|
| 0.07 | 0.0 | 0.0 | 0.0 | 0.111687 | 0.848151 |
| | 5.5 | 0.0 | 0.0 | 0.303608 | 0.693641 |
| | 12.5 | 0.0 | 0.0 | 0.665827 | 0.450229 |
| | 25.0 | −0.354662 | 1.416299 | 3.925792 | −3.814382 |
| 0.20 | 0.0 | 0.0 | 0.0 | 0.152862 | 0.78183 |
| | 5.5 | 0.0 | 0.0 | 0.35057 | 0.60962 |
| | 12.5 | 0.0 | 0.0 | 0.691757 | 0.407027 |
| | 25.0 | 0.0 | 1.534332 | −17.32797 | 14.40045 |
| 0.50 | 0.0 | 0.0 | 0.0 | 0.251497 | 0.705487 |
| | 5.5 | 0.0 | 0.0 | 0.661656 | 0.348831 |
| | 12.5 | 0.0 | 0.0 | 1.601127 | −0.424487 |
| | 25.0 | 2.743878 | −18.09787 | 13.731616 | 2.08857 |
| 0.70 | 0.0 | 0.0 | 0.0 | 0.280233 | 0.697339 |
| | 5.5 | 0.0 | 0.0 | 0.693236 | 0.346922 |
| | 12.5 | 0.0 | 0.0 | 1.566717 | −0.325088 |
| | 25.0 | −1.213787 | 6.301881 | 4.370901 | −6.988637 |
| 0.80 | 0.0 | 0.0 | 0.0 | 0.338131 | 0.637794 |
| | 5.5 | 0.0 | 0.0 | 0.719554 | 0.349286 |
| | 12.5 | 0.0 | 0.0 | 1.373569 | −0.175915 |
| | 25.0 | −0.403791 | 1.579764 | 5.205654 | −4.533334 |
| 0.90 | 0.0 | 0.0 | 0.0 | 0.436478 | 0.555708 |
| | 5.5 | 0.0 | −0.155809 | 1.523391 | −0.266623 |
| | 12.5 | 0.0 | −0.217166 | 2.2467 | −0.855572 |
| | 25.0 | 0.0 | −0.733177 | 6.203364 | −3.94136 |
| 0.93 | 0.0 | 0.0 | 0.0 | 0.464299 | 0.535423 |
| | 5.5 | 0.0 | −0.17031 | 1.579231 | −0.294406 |
| | 12.5 | 0.0 | −0.235091 | 2.28368 | −0.853961 |
| | 25.0 | 0.0 | −0.62338 | 5.154261 | −3.165345 |

Coefficients for the equations of the normalized $Cp$ as a function of frontal aspect ratio $far < 1.0$: $Cpnorm_{pad,\,zh}(far) = a_0 + a_1(far)$

| $pad$ | $zh$ | $a_1$ | $a_0$ |
|---|---|---|---|
| 0.0 | 0.07 | 0.21 | 0.79 |
| | 0.20 | 0.166 | 0.834 |
| | 0.40 | 0.102 | 0.898 |
| | 0.60 | 0.066 | 0.934 |
| | 0.80 | −0.04 | 1.04 |
| | 0.93 | −0.292 | 1.292 |

(*continued*)

TABLE (*continued*)

| *pad* | *zh* | $a_1$ | $a_0$ |
|---|---|---|---|
| 5.0 | 0.07 | 0.286 | 0.714 |
| | 0.20 | 0.21 | 0.79 |
| | 0.40 | 0.148 | 0.852 |
| | 0.60 | 0.156 | 0.844 |
| | 0.80 | 0.028 | 0.972 |
| | 0.93 | −0.364 | 1.364 |
| 7.5 | 0.07 | 0.134 | 0.866 |
| | 0.20 | 0.12 | 0.88 |
| | 0.40 | 0.054 | 0.946 |
| | 0.60 | 0.6245004e-17 | 1.0 |
| | 0.80 | 0.038 | 0.962 |
| | 0.93 | −0.352 | 1.352 |
| 10.0 | 0.07 | 0.182 | 0.818 |
| | 0.20 | 0.046 | 0.954 |
| | 0.40 | −0.12 | 1.12 |
| | 0.60 | −0.166 | 1.166 |
| | 0.80 | −0.052 | 1.052 |
| | 0.93 | −0.428 | 1.428 |
| 12.5 | 0.07 | 0.1 | 0.9 |
| | 0.20 | −0.068 | 1.068 |
| | 0.40 | −0.058 | 1.058 |
| | 0.60 | −0.044 | 1.044 |
| | 0.80 | 0.032 | 0.968 |
| | 0.93 | −0.334 | 1.334 |

Coefficients for the equations of the normalized *Cp* as a function of frontal aspect ratios $far > 1.0$: $Cpnorm_{pad,\,zh}(far) = \left\{a_1 far + \frac{a_2}{far} + a_3\right\}^{1/2}$

| *pad* | *zh* | $a_1$ | $a_2$ | $a_3$ |
|---|---|---|---|---|
| 0.0 | 0.07 | −0.070887 | 0.335565 | 0.741492 |
| | 0.20 | −0.061746 | 0.39232 | 0.670057 |
| | 0.40 | −0.071734 | 0.370249 | 0.700161 |
| | 0.60 | −0.075213 | 0.280472 | 0.799646 |
| | 0.80 | −0.081452 | 0.261036 | 0.821341 |
| | 0.93 | −0.05991 | 0.441293 | 0.620374 |
| 5.0 | 0.07 | −0.625867 | −3.31499 | 4.938818 |
| | 0.20 | −0.700802 | −3.691923 | 5.39902 |
| | 0.40 | −0.551417 | −2.657088 | 4.208561 |
| | 0.60 | −0.394759 | −1.857109 | 3.243966 |
| | 0.80 | −0.384892 | −1.582766 | 2.964682 |
| | 0.93 | −0.471534 | −1.938719 | 3.408053 |
| 7.5 | 0.07 | −0.464735 | −4.370468 | 5.827134 |
| | 0.20 | −0.484764 | −4.700937 | 6.175447 |
| | 0.40 | −0.357666 | −3.421083 | 4.761667 |
| | 0.60 | −0.430568 | −3.272576 | 4.686477 |
| | 0.80 | −0.538978 | −3.080677 | 4.608249 |
| | 0.93 | −0.295157 | −2.106807 | 3.39147 |
| 10.0 | 0.07 | −0.445623 | −5.965503 | 7.414155 |
| | 0.20 | −0.562911 | −8.352512 | 9.919405 |
| | 0.40 | −0.303556 | −5.104654 | 6.409214 |
| | 0.60 | −0.396287 | −4.685712 | 6.096834 |
| | 0.80 | −0.326486 | −3.146084 | 4.485651 |
| | 0.93 | −0.491857 | −3.607476 | 5.109896 |

(*continued*)

TABLE (*continued*)

| *pad* | *zh* | $a_1$ | $a_2$ | $a_3$ |
|---|---|---|---|---|
| 12.5 | 0.07 | 0.39952 | −6.357705 | 6.938206 |
| | 0.20 | 0.560605 | −10.512008 | 10.939653 |
| | 0.40 | 0.460531 | −5.146305 | 5.668398 |
| | 0.60 | 0.052937 | −4.346084 | 5.273574 |
| | 0.80 | −0.17023 | −3.285382 | 4.448491 |
| | 0.93 | −0.489256 | −4.363034 | 5.840238 |

Coefficients for the equations of the normalized *Cp* as a function of side aspect ratio $sar < 1.0$: $Cpnorm_{pad,zh}(sar) = a_0 + a_1(sar)$

| *pad* | *zh* | $a_1$ | $a_0$ |
|---|---|---|---|
| 0.0 | 0.07 | −0.022 | 1.022 |
| | 0.20 | 0.056 | 0.944 |
| | 0.40 | −0.03 | 1.03 |
| | 0.60 | 6.245004e-17 | 1.0 |
| | 0.80 | −0.02 | 1.02 |
| | 0.93 | −0.166 | 1.166 |
| 5.0 | 0.07 | 0.172 | 0.828 |
| | 0.20 | 0.19 | 0.81 |
| | 0.40 | 0.334 | 0.666 |
| | 0.60 | 0.438 | 0.562 |
| | 0.80 | 0.31 | 0.69 |
| | 0.93 | −0.09 | 1.09 |
| 7.5 | 0.07 | 0.266 | 0.734 |
| | 0.20 | 0.298 | 0.702 |
| | 0.40 | 0.46 | 0.54 |
| | 0.60 | 0.436 | 0.564 |
| | 0.80 | 0.324 | 0.676 |
| | 0.93 | −0.118 | 1.118 |
| 10.0 | 0.07 | 0.328 | 0.672 |
| | 0.20 | 0.318 | 0.682 |
| | 0.40 | 0.8 | 0.2 |
| | 0.60 | 0.666 | 0.334 |
| | 0.80 | 0.206 | 0.794 |
| | 0.93 | −0.286 | 1.286 |
| 12.5 | 0.07 | 0.75 | 0.25 |
| | 0.20 | 1.104 | −0.104 |
| | 0.40 | 1.428 | −0.428 |
| | 0.60 | 1.2 | −0.2 |
| | 0.80 | 0.634 | 0.366 |
| | 0.93 | 6.245004e-17 | 1.0 |

Coefficients for the equations of the normalized *Cp* as a function of side aspect ratio $sar > 1.0$: $Cpnorm_{pad,zh}(sar) = \left\{a_1 sar + \frac{a_2}{sar} + a_3\right\}^{1/2}$

| *pad* | *zh* | $a_1$ | $a_2$ | $a_3$ |
|---|---|---|---|---|
| 0.0 | 0.07 | 0.102648 | 0.307944 | 0.589408 |
| | 0.20 | −0.044242 | −0.132726 | 1.176968 |
| | 0.40 | −0.02005 | −0.06015 | 1.0802 |
| | 0.60 | −2.751206e-10 | −5.399712e-10 | 1.0 |
| | 0.80 | −0.127266 | −0.101574 | 1.22884 |
| | 0.93 | 0.175931 | 0.527814 | 0.296255 |

(*continued*)

TABLE (*continued*)

| *pad* | *zh* | $a_1$ | $a_2$ | $a_3$ |
|---|---|---|---|---|
| 5.0 | 0.07 | −0.61983 | −2.745612 | 4.365442 |
| | 0.20 | −0.455586 | −2.714454 | 4.17004 |
| | 0.40 | 0.01539 | −1.522998 | 2.507608 |
| | 0.60 | 8.495999e-03 | −1.108008 | 2.099512 |
| | 0.80 | 0.03363 | −0.665862 | 1.632232 |
| | 0.93 | −0.83599 | −2.639028 | 4.475018 |
| 7.5 | 0.07 | −0.672534 | −4.465068 | 6.137602 |
| | 0.20 | −0.589638 | −4.571604 | 6.161242 |
| | 0.40 | 0.44217 | −2.377428 | 2.935258 |
| | 0.60 | 0.313214 | −2.334822 | 3.021608 |
| | 0.80 | 0.53643 | −1.011222 | 1.474792 |
| | 0.93 | −0.32829 | −2.984262 | 4.312552 |
| 10.0 | 0.07 | −1.31805 | −7.924662 | 10.242712 |
| | 0.20 | −2.14576 | −11.416512 | 14.562272 |
| | 0.40 | 0.0608 | −6.2016 | 7.1408 |
| | 0.60 | 0.699422 | −3.950934 | 4.251512 |
| | 0.80 | 0.51795 | −2.521878 | 3.003928 |
| | 0.93 | −1.627836 | −6.191754 | 8.81959 |
| 12.5 | 0.07 | 1.15625 | −5.8125 | 5.65625 |
| | 0.20 | 0.811914 | −10.848372 | 11.036458 |
| | 0.40 | 3.144588 | −2.954106 | 0.809518 |
| | 0.60 | 3.525422 | −0.048534 | −2.476888 |
| | 0.80 | 1.802288 | −0.832296 | 0.030008 |
| | 0.93 | −0.384444 | −4.326666 | 5.71111 |

Coefficients for the equations of the normalized *Cp*: horizontal distribution vs. wind direction: $Cpnorm_{zh,\,anw}(xl) = a_0 + a_1(xl) + a_2(xl)^2 + a_3(xl)^3$

| *zh* | *anw* (°) | $a_3$ | $a_2$ | $a_1$ | $a_0$ |
|---|---|---|---|---|---|
| 0.50 | 0.0 | 0.0 | −3.04662 | 3.04662 | 0.268462 |
| | 10.0 | 0.0 | −3.142447 | 2.873329 | 0.38632 |
| | 20.0 | 0.0 | −2.001162 | 1.398438 | 0.693916 |
| | 30.0 | 0.0 | −1.275862 | 0.278803 | 0.935081 |
| | 40.0 | 0.0 | −1.058275 | −0.01627 | 0.871259 |
| | 50.0 | 0.0 | −0.891626 | 0.247508 | 0.428414 |
| | 60.0 | 0.0 | −1.560755 | 1.496049 | −0.257573 |
| | 70.0 | 0.0 | −1.990676 | 2.614312 | −0.994965 |
| | 80.0 | 0.0 | −1.651067 | 2.530479 | −1.359928 |
| | 90.0 | −5.984848 | 10.036713 | −3.883683 | −0.778811 |
| 0.70 | 0.0 | 0.0 | −2.501166 | 2.501166 | 0.401189 |
| | 10.0 | 0.0 | −2.665435 | 2.355141 | 0.523287 |
| | 20.0 | 0.0 | −1.674825 | 1.008462 | 0.802867 |
| | 30.0 | 0.0 | −0.869048 | −0.176541 | 1.051723 |
| | 40.0 | 0.0 | −0.635198 | −0.467529 | 0.973357 |
| | 50.0 | 0.0 | −0.667077 | 3.841881e-03 | 0.485571 |
| | 60.0 | 0.0 | −1.415846 | 1.367316 | −0.231142 |
| | 70.0 | 0.0 | −2.064103 | 2.719557 | −1.005524 |
| | 80.0 | 0.0 | −1.842775 | 2.788363 | −1.37687 |
| | 90.0 | −4.015152 | 6.670746 | −2.319231 | −0.836434 |

(*continued*)

TABLE (*continued*)

| *zh* | *anw* (°) | $a_3$ | $a_2$ | $a_1$ | $a_0$ |
|---|---|---|---|---|---|
| 0.90 | 0.0 | 0.0 | −2.456876 | 2.456876 | 0.451469 |
| | 10.0 | 0.0 | −2.681034 | 2.335446 | 0.581156 |
| | 20.0 | 0.0 | −1.724942 | 0.981305 | 0.888531 |
| | 30.0 | 0.0 | −0.832512 | −0.270429 | 1.118564 |
| | 40.0 | 0.0 | −0.547786 | −0.544942 | 0.992378 |
| | 50.0 | 0.0 | −0.88711 | 0.279757 | 0.426546 |
| | 60.0 | 0.0 | −1.85509 | 1.935973 | −0.375921 |
| | 70.0 | 0.0 | −2.815851 | 3.659487 | −1.236923 |
| | 80.0 | 0.0 | −2.449507 | 3.577449 | −1.585214 |
| | 90.0 | −6.959984 | 10.745338 | −3.502836 | −0.877273 |

*Coefficients for the curve-fitting equations — Leeward side*

Polynomial function for the reference *Cp* (eqn. (7)):

$$Cp_{ref}(zh) = -0.079239zh^3 + 0.542317zh^2 - 0.496769zh - 0.331533$$

Coefficients for the equations of the normalized *Cp* as a function of environmental and geometrical parameters as follows:

Coefficients for the equations of the normalized *Cp* as a function of terrain roughness: $Cpnorm_{zh}(\alpha) = a_0 + a_1(\alpha) + a_2(\alpha)^2$

| *zh* | $a_2$ | $a_1$ | $a_0$ |
|---|---|---|---|
| 0.1 | −14.368685 | 4.520431 | 0.0667639 |
| 0.3 | −13.490491 | 4.101437 | 0.706052 |
| 0.5 | −8.775919 | 1.322245 | 1.088822 |
| 0.7 | −4.662405 | −0.929782 | 1.395398 |
| 0.9 | 2.382908 | −4.837467 | 1.940878 |

Coefficients for the equations of the normalized *Cp* as a function of density of surrounding buildings: $Cpnorm_{zh}(pad) = a_0 + a_1(pad) + a_2(pad)^2 + a_3(pad)^3 + a_4(pad)^4 + a_5(pad)^5$

| *zh* | $a_5$ | $a_4$ | $a_3$ | $a_2$ | $a_1$ | $a_0$ |
|---|---|---|---|---|---|---|
| 0.07 | 9.118209e-08 | −1.050363e-05 | 3.932533e-04 | −4.734698e-03 | −0.015304 | 1.047295 |
| 0.20 | 5.934754e-08 | −6.708652e-06 | 2.340744e-04 | −1.943067e-03 | −0.031483 | 1.043295 |
| 0.40 | 5.052791e-08 | −5.537346e-06 | 1.722449e-04 | −3.926684e-04 | −0.046517 | 1.034663 |
| 0.60 | 5.595805e-08 | −6.121612e-06 | 1.8897e-04 | −3.177597e-04 | −0.051446 | 1.032759 |
| 0.80 | 5.553558e-08 | −5.931215e-06 | 1.719758e-04 | 3.013991e-04 | −0.059971 | 1.037969 |
| 0.93 | 6.211419e-08 | −6.759794e-06 | 2.024378e-04 | 1.182029e-04 | −0.065764 | 1.033975 |

Coefficients for the equations of the normalized *Cp* as a function of height of surrounding buildings: $Cpnorm_{zh,pad}(rbh) = a_0 + a_1(rbh) + a_2(rbh)^2$

| *zh* | *pad* | $a_2$ | $a_1$ | $a_0$ |
|---|---|---|---|---|
| 0.07 | 0.00 | 0.0 | 0.547959 | 0.465538 |
| | 5.00 | 0.0 | 0.625743 | 0.308268 |
| | 6.25 | 0.0 | 0.859533 | 0.107587 |
| | 12.50 | 0.0 | 1.710552 | −0.681624 |

(*continued*)

TABLE (*continued*)

| *zh* | *pad* | $a_2$ | $a_1$ | $a_0$ |
|---|---|---|---|---|
| 0.20 | 0.00 | 0.0 | 0.473757 | 0.527487 |
| | 5.00 | 0.0 | 0.636732 | 0.294108 |
| | 6.25 | 0.123639 | 0.432008 | 0.44064 |
| | 12.50 | 0.080103 | 1.471191 | −0.547645 |
| 0.40 | 0.00 | −0.043739 | 0.599345 | 0.427938 |
| | 5.00 | 0.054539 | 0.299349 | 0.645489 |
| | 6.25 | 0.100427 | 0.35117 | 0.483096 |
| | 12.50 | 0.175853 | 0.568029 | 0.223168 |
| 0.60 | 0.00 | −0.069086 | 0.793503 | 0.287883 |
| | 5.00 | 0.029377 | 0.402683 | 0.594877 |
| | 6.25 | 0.066082 | 0.524015 | 0.376383 |
| | 12.50 | 0.145046 | 0.567979 | 0.264523 |
| 0.80 | 0.00 | −0.036376 | 0.781825 | 0.258777 |
| | 5.00 | 0.011009 | 0.55164 | 0.435343 |
| | 6.25 | −1.58012e-03 | 1.127839 | −0.084281 |
| | 12.50 | 0.09395 | 1.114736 | −0.111437 |
| 0.93 | 0.00 | 2.138076e-03 | 0.655048 | 0.38064 |
| | 5.00 | 0.03126 | 0.526521 | 0.418668 |
| | 6.25 | 0.102993 | 0.946754 | −0.122071 |
| | 12.50 | 0.202243 | 1.119405 | −0.353569 |

Coefficients for the equations of the normalized *Cp* as a function of frontal aspect ratio $far < 1$: $Cpnorm_{pad,\,zh}(far) = a_0 + a_1(far)$

| *pad* | *zh* | $a_1$ | $a_0$ |
|---|---|---|---|
| 0.0 | 0.07 | 0.77 | 0.23 |
| | 0.20 | 0.694 | 0.306 |
| | 0.40 | 0.624 | 0.376 |
| | 0.60 | 0.6 | 0.4 |
| | 0.80 | 0.666 | 0.334 |
| | 0.93 | 0.55 | 0.45 |
| 5.0 | 0.07 | 1.31 | −0.31 |
| | 0.20 | 1.096 | −0.096 |
| | 0.40 | 1.048 | −0.048 |
| | 0.60 | 1.096 | −0.096 |
| | 0.80 | 1.142 | −0.142 |
| | 0.93 | 1.042 | −0.042 |
| 7.5 | 0.07 | 1.32 | −0.32 |
| | 0.20 | 1.17 | −0.17 |
| | 0.40 | 1.142 | −0.142 |
| | 0.60 | 1.17 | −0.17 |
| | 0.80 | 1.292 | −0.292 |
| | 0.93 | 1.25 | −0.25 |
| 10.0 | 0.07 | 1.302 | −0.302 |
| | 0.20 | 1.166 | −0.166 |
| | 0.40 | 1.12 | −0.12 |
| | 0.60 | 1.25 | −0.25 |
| | 0.80 | 1.428 | −0.428 |
| | 0.93 | 1.428 | −0.428 |
| 12.5 | 0.07 | 1.366 | −0.366 |
| | 0.20 | 1.174 | −0.174 |
| | 0.40 | 1.166 | −0.166 |
| | 0.60 | 1.244 | −0.244 |
| | 0.80 | 1.4 | −0.4 |
| | 0.93 | 1.412 | −0.412 |

Coefficients for the equations of the normalized $Cp$ as a function of frontal aspect ratio $far > 1.0$: $Cpnorm_{pad,zh}(far) = \left\{a_1 far + \frac{a_2}{far} + a_3\right\}^{1/2}$

| *pad* | *zh* | $a_1$ | $a_2$ | $a_3$ |
|---|---|---|---|---|
| 0.0 | 0.07 | 0.391319 | 0.275277 | 0.305879 |
| | 0.20 | 0.208852 | 0.045117 | 0.727577 |
| | 0.40 | 0.176644 | 0.135403 | 0.657545 |
| | 0.60 | 0.222872 | 0.219437 | 0.5177 |
| | 0.80 | 0.352525 | 0.51124 | 0.095033 |
| | 0.93 | 0.409298 | 0.101415 | 0.461285 |
| 5.0 | 0.07 | 0.313066 | 1.29096 | −0.679717 |
| | 0.20 | 0.262845 | 1.187068 | −0.511316 |
| | 0.40 | 0.198393 | 0.852449 | −0.107538 |
| | 0.60 | 0.202255 | 0.824728 | −0.109405 |
| | 0.80 | 0.266436 | 0.989084 | −0.34636 |
| | 0.93 | 0.378433 | 0.831703 | −0.27258 |
| 7.5 | 0.07 | 0.355636 | 1.865418 | −1.293254 |
| | 0.20 | 0.256393 | 1.501845 | −0.83996 |
| | 0.40 | 0.195066 | 1.248485 | −0.513001 |
| | 0.60 | 0.179345 | 1.132885 | −0.406631 |
| | 0.80 | 0.248347 | 1.426085 | −0.79038 |
| | 0.93 | 0.286457 | 1.200878 | −0.562477 |
| 10.0 | 0.07 | 0.162696 | 1.401255 | −0.650645 |
| | 0.20 | 0.14259 | 1.382313 | −0.611037 |
| | 0.40 | 0.072493 | 1.036706 | −0.199349 |
| | 0.60 | 0.062272 | 0.956828 | −0.131138 |
| | 0.80 | 0.116832 | 1.191314 | −0.445541 |
| | 0.93 | 0.111723 | 0.959598 | −0.190495 |
| 12.5 | 0.07 | 0.187639 | 1.532033 | −0.830662 |
| | 0.20 | 0.113114 | 1.30869 | −0.518821 |
| | 0.40 | 0.090391 | 1.096843 | −0.281639 |
| | 0.60 | 0.058215 | 0.921987 | −0.086177 |
| | 0.80 | 0.138563 | 1.304438 | −0.561468 |
| | 0.93 | 0.115601 | 1.108345 | −0.337801 |

Coefficients for the equations of the normalized $Cp$ as a function of side aspect ratio $sar < 1.0$: $Cpnorm_{pad,zh}(sar) = a_0 + a_1(sar)$

| *pad* | *zh* | $a_1$ | $a_0$ |
|---|---|---|---|
| 0.0 | 0.07 | −0.462 | 1.462 |
| | 0.20 | −0.444 | 1.444 |
| | 0.40 | −0.5 | 1.5 |
| | 0.60 | −0.6 | 1.6 |
| | 0.80 | −0.666 | 1.666 |
| | 0.93 | −0.986 | 1.986 |
| 5.0 | 0.07 | 0.62 | 0.38 |
| | 0.20 | 0.484 | 0.516 |
| | 0.40 | 0.286 | 0.714 |
| | 0.60 | 0.322 | 0.678 |
| | 0.80 | 0.358 | 0.642 |
| | 0.93 | 0.124 | 0.876 |
| 7.5 | 0.07 | 0.56 | 0.44 |
| | 0.20 | 0.416 | 0.584 |
| | 0.40 | 0.358 | 0.642 |
| | 0.60 | 0.378 | 0.622 |
| | 0.80 | 0.416 | 0.584 |
| | 0.93 | 6.245004e-17 | 1.0 |

(*continued*)

TABLE (*continued*)

| *pad* | *zh* | $a_1$ | $a_0$ |
|---|---|---|---|
| 10.0 | 0.07 | 0.418 | 0.582 |
| | 0.20 | 0.374 | 0.626 |
| | 0.40 | 0.28 | 0.72 |
| | 0.60 | 0.334 | 0.666 |
| | 0.80 | 0.286 | 0.714 |
| | 0.93 | 0.058 | 0.942 |
| 12.5 | 0.07 | 0.586 | 0.414 |
| | 0.20 | 0.392 | 0.608 |
| | 0.40 | 0.208 | 0.792 |
| | 0.60 | 0.088 | 0.912 |
| | 0.80 | 0.2 | 0.8 |
| | 0.93 | −0.118 | 1.118 |

Coefficients for the equations of the normalized *Cp* as a function of side aspect ratio $sar > 1.0$: $Cpnorm_{pad,zh}(sar) = \left\{a_1 sar + \frac{a_2}{sar} + a_3\right\}^{1/2}$

| *pad* | *zh* | $a_1$ | $a_2$ | $a_3$ |
|---|---|---|---|---|
| 0.0 | 0.07 | 1.549121 | 4.008955 | −4.558076 |
| | 0.20 | 1.293432 | 3.376296 | −3.669728 |
| | 0.40 | 0.818276 | 2.757414 | −2.575691 |
| | 0.60 | 0.622491 | 2.463733 | −2.086225 |
| | 0.80 | 0.431822 | 2.206986 | −1.638808 |
| | 0.93 | 1.15475 | 3.567738 | −3.722488 |
| 5.0 | 0.07 | 1.234668 | 3.821814 | −4.056482 |
| | 0.20 | 1.086419 | 3.381557 | −3.467976 |
| | 0.40 | 1.110227 | 3.330677 | −3.440903 |
| | 0.60 | 1.248462 | 3.745386 | −3.993848 |
| | 0.80 | 1.158504 | 3.817008 | −3.975512 |
| | 0.93 | 0.924129 | 3.214321 | −3.13845 |
| 7.5 | 0.07 | 1.6176 | 4.7352 | −5.352801 |
| | 0.20 | 1.405914 | 4.082196 | −4.48811 |
| | 0.40 | 1.39227 | 4.047642 | −4.439912 |
| | 0.60 | 1.446764 | 4.209078 | −4.655842 |
| | 0.80 | 1.541118 | 4.623354 | −5.164472 |
| | 0.93 | 1.395 | 4.185 | −4.58 |
| 10.0 | 0.07 | 1.728091 | 5.065453 | −5.793544 |
| | 0.20 | 1.675056 | 4.762584 | −5.437641 |
| | 0.40 | 1.632 | 4.6368 | −5.2688 |
| | 0.60 | 1.623354 | 4.746708 | −5.370063 |
| | 0.80 | 2.133661 | 5.767382 | −6.900996 |
| | 0.93 | 2.099225 | 5.670099 | −6.769291 |
| 12.5 | 0.07 | 2.249115 | 6.239501 | −7.488376 |
| | 0.20 | 2.121972 | 5.826368 | −6.948252 |
| | 0.40 | 1.99874 | 5.578012 | −6.576709 |
| | 0.60 | 2.373076 | 6.268238 | −7.641063 |
| | 0.80 | 2.133851 | 5.94792 | −7.081692 |
| | 0.93 | 2.204859 | 6.021059 | −7.225708 |

Coefficients for the equations of the normalized *Cp*: horizontal distribution vs. wind direction: $Cpnorm_{zh,\,anw}(xl) = a_0 + a_1(xl) + a_2(xl)^2 + a_3(xl)^3 + a_4(xl)^4$

| *zh* | *anw* (°) | $a_4$ | $a_3$ | $a_2$ | $a_1$ | $a_0$ |
|---|---|---|---|---|---|---|
| 0.50 | 90.0 | 0.0 | 9.325952 | −16.031002 | 6.08061 | 2.162909 |
| | 110.0 | 0.0 | 2.526807 | −5.145221 | 3.28289 | 1.400238 |
| | 130.0 | 0.0 | 0.200855 | −1.520047 | 1.734472 | 1.275364 |
| | 160.0 | 0.0 | 0.861888 | −1.966841 | 1.561282 | 0.923007 |
| | 180.0 | 0.0 | 4.145989e-16 | −0.107692 | 0.107692 | 0.975846 |
| 0.70 | 90.0 | 0.0 | 11.862859 | −19.086364 | 6.79763 | 2.204853 |
| | 110.0 | 0.0 | 1.79934 | −2.526981 | 1.326103 | 1.631755 |
| | 130.0 | 0.0 | −0.069542 | 0.404196 | 0.124611 | 1.506259 |
| | 160.0 | 0.0 | 1.003108 | −0.873077 | 0.398465 | 1.093671 |
| | 180.0 | 0.0 | 3.88578e-16 | 0.449883 | −0.449883 | 1.102028 |
| 0.90 | 90.0 | −13.234266 | 47.482906 | −48.637238 | 13.933178 | 2.493133 |
| | 110.0 | −18.269231 | 38.486402 | −24.083741 | 4.338003 | 1.973497 |
| | 130.0 | −9.985431 | 17.831974 | −8.056789 | 0.346156 | 1.844014 |
| | 160.0 | −8.458625 | 17.902681 | −10.191521 | 1.433689 | 1.232881 |
| | 180.0 | −6.555944 | 13.106061 | −7.364394 | 0.809767 | 1.244049 |